ELECTROLYTIC PRODUCTION OF ALUMINIUM: FUNDAMENTAL AND APPLIED STUDIES ON THE EFFECT OF ANODE COMPOSITION ON THE ANODE-ELECTROLYTE INTERFACIAL CONDITIONS.

by

J.A. OSBORNE. B.Sc. (Hons.), (Tas.)

being a Thesis submitted in fulfilment of the requirements for the Degree of

Master of Science

UNIVERSITY OF TASMANIA

HOBART.

(May 1968)

DECLARATION OF ORIGINALITY

All of the experimental work in this thesis, except where directly ascribed to others, has been performed solely by the author. No part of the text has previously been submitted for any other degree or diploma in any University, nor does it contain, to the best knowledge of the undersigned, any material which has been published by others, except where due reference has been so made.

SUMMARY

This thesis deals with a study of the wettability of amorphous carbon, of the type employed as anode material in the production of aluminium, by cryolite-based solutions. The wettability of carbon has been improved by the addition of inorganic additives of the type used in cryolite electrolytes, such as aluminium oxide, calcium fluoride and carbonate, and lithium fluoride and carbonate.

Particular improvements in carbon wettability are noted when the system is contained in an atmosphere of carbon dioxide - carbon monoxide, corresponding to practical production conditions.

Furtheremore, when anodes prepared containing these additives are used in a laboratory aluminium cell, notable reductions in cell voltage are achieved at practical anode current densities. The improved adhesion of the two phases has also been demonstrated by measurement of the current density and voltage conditions required to induce anode effects in this cell.

Improvements in power requirements and carbon consumption per unit weight of product are shown, and finally, an assessment of the project potential under industrial operating conditions has been made.

TABLE OF CONTENTS

Table of Contents continued.

INTRODUCTION:

The work described herein was undertaken primarily as an applied industrial study at the Comalco Aluminium (Bell Bay) Limited aluminium smelter. The overall object was the lowering of the individual reduction cell voltage as a means of improving the energy efficiency of the Hall-Heroult electrolytic process for the manufacture of aluminium and its alloys.

It is well known in the aluminium industry that the electrolysis voltage required to deposit aluminium from a cryolite-based electrolyte is in practice of the order of 4 to 5 volts. This compares with theoretical values of between 1.01V and 2.22V (1) depending on the type of electrodes and overall reactions that are assumed.

The following theoretical reversible decomposition potentials at 1000°C with the reactants in their standard states have been found:

1.01V for the reaction

$$Al_2O_3 + 3C = 2Al + 3CO \qquad \text{(Ref. 1)},$$

and 1.16V for the reaction

$$Al_2O_3 + \tfrac{3}{2}C = 2Al + \tfrac{3}{2}CO_2 \qquad \text{(Ref. 1)};$$

from thermodynamic data, we have 2.22V for the reaction

$$Al_2O_3(s) = 2Al(l) + \tfrac{3}{2}O_2(g) \qquad \text{(Ref. 1)}.$$

In practice the decomposition voltage lies between 1.45 and 1.65V, the overvoltage being mainly anodic (2).

While a certain amount of the excess energy, at the high currents used industrially, is necessary to maintain the electrolyte in a molten condition at its operating temperature (of the order of 980°C), it can be seen, as various workers (3,4,5) have shown, that a significant factor in the energy requirements is the anode overvoltage. Although conflicting explanations exist as to the mechanism of this overvoltage, typical figures at practical current densities, alumina concentrations, and cell temperatures are of the order of 0.4 - 0.7v.

In an aluminium reduction cell the operating process normally consists of the continuous downward feeding of a carbonaceous anode, comprising a petroleum coke/pitch mixture, into a molten bath of a mixture of cryolite, aluminium oxide, and calcium fluoride. This molten electrolyte is contained in a carbon-lined steel shell, which acts as the cathode.

At the anode, the two surfaces directly in contact with each other are the carbon electrode and the cryolitic electrolyte. Structurally, these two materials are profoundly dissimilar, the former consisting of a covalent solid, with a varying degree of graphitic structure, and the latter consisting of an ionic melt. One result of this structural difference is a marked lack of physical adhesion or wettability under certain

atmospheric environments (6), which manifests itself in an imperfect electrical contact. This contributes to a higher voltage than is desirable under plant operating conditions.

In addition to the overvoltage produced in an operating cell, the slow release of the primary anode product, CO_2, allows the formation of significant amounts of carbon monoxide, resulting in a carbon usage of approximately 0.5 lb. for every one pound of aluminium produced, compared with a theoretical usage of 0.33 lb. of carbon for the reaction:-

$$2Al_2O_3 + 3C = 4Al + 3CO_2$$

Therefore if improved physical and electrical contact can be established between the two interfacial surfaces, a lower total voltage drop per cell can be expected. Also, if a more rapid release of anode gases can be realised, a reduction in carbon consumption can be expected.

The experimental route chosen for this project has been to study the effect of incorporating small amounts of inorganic additives to the unbaked carbon mixture. These additives have been chosen to promote the contact between anode and electrolyte. Because of the applied nature of this work, the choice of additive materials has been restricted to those which are compatible with the normal industrial production of aluminium. Such

compounds include aluminium oxide, calcium fluoride, calcium carbonate, aluminium fluoride, and certain lithium compounds.

The study of the use of these compounds is described in the subsequent two major sections:-

(i) Contact Angle Studies

(ii) Laboratory Reduction Cell Studies.

From the point of view of both local application and experimental technique, only baked anodes were studied. Although similar additives could be made to Soderberg electrodes, this aspect was not investigated, as such, in this work.

PART I : CONTACT ANGLE STUDIES

(a) General:

When a drop of liquid rests under equilibrium on a horizontal solid surface, a configuration of the following type is adopted:-

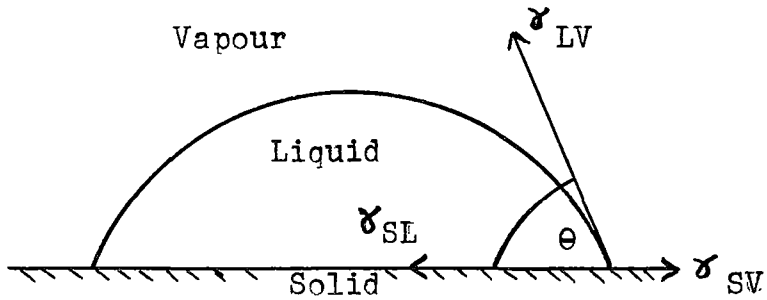

In such a system, the interfacial surface tensions are related by the following expression:-

$$\gamma_{SV} - \gamma_{SL} = \gamma_{LV} \cos \theta$$

where γ_{SV}, γ_{SL}, and γ_{LV} refer to the solid-vapour, solid-liquid, and liquid-vapour surface tensions respectively, and θ is the contact angle formed by the liquid drop on the surface in a given atmosphere. This angle may be measured geometrically.

Although experimental difficulties exist for the measurement of the various surface tensions, and stresses on the solid surface would confer non-equilibrium properties on the system, the measurement of θ is able to provide valuable information as to the relationships and affinities between the three phases.

In particular, in the absence of chemical reactions at the interfaces, the shape of the liquid drop, and

hence the value of the contact angle, enables one to make an assessment of the "wettability" of the solid by the liquid. All solids are wet by all liquids to some extent, i.e., $\theta < 180^{\circ}$; the greater the tendency of the liquid to spread on the solid, the smaller will θ become. When the liquid spreads completely over the solid, then θ equals zero.

In the present study, attention has been directed to the wettability of baked amorphous carbon surfaces by liquid cryolite and its various alumina-containing solutions. It has been the intention to measure the extent of wettability as a function of carbon composition, particularly as affected by the addition of the inorganic additives related to the alumina reduction process.

The work of Vajna (6) has been followed up and used as a basis for further study, as described in detail in the following sections.

(b) Experimental:

(i) Anode Preparation

"Green", or unbaked, anodes were prepared on a laboratory scale by a method analagous to plant operation. Initially, this consisted of preparing a quantity of dry petroleum coke of the following particle size analysis:-

-	¾ + 4 mesh	17%
-	4 + 20 mesh	33%
-	20 + 48 mesh	7%
-	48 + 100 mesh	8%
-	100 + 200 mesh	13%
-	200 mesh	22%

Tyler Sieves

These percentages were selected from plant records over a twelve month period, and thus constituted a particle size distribution which had proved satisfactory in reduction furnace operation.

A pre-determined quantity of the above coke mixture was heated to approximately 100°C in a two-gallon double sigma-bladed Baker-Perkins mixer, and 20% of its weight of coal-tar pitch, of softening point 105 - 110°C, added.

Maintaining parity with plant conditions, the pitch-coke mixture was heated to 125°C, and a suitable quantity, normally 150 - 160 grams transferred to a steel mould, 2" inside diameter and 3" long, lagged

with refractory paper, maintained at the same temperature. By means of a suitable plunger (See Fig.1), the hot mixture was compressed to a total pressure of 17,500 - 18,000 lb, or 5,570 - 5,730 lb per square inch, using a Mohr and Federhaff Universal Testing Machine. The pressed block was then extruded from the mould for further study.

When inorganic additives were incorporated into the anode mixture, they were added in the form of a fine powder, the content being based on the weight of petroleum coke in the carbonaceous mixture.

Modifications to the petroleum coke size distribution were made when small surface irregularities were obtained in the anodes, caused by the $-\frac{3}{4}$ + 4 mesh solids fraction. By screening out this fraction from all but the earliest trial anodes, a coke particle size distribution was obtained as follows:-

- 4 + 20 mesh	approx. 40%	Tyler sieves
- 20 + 48 mesh	approx. 8%	
- 48 + 100 mesh	approx. 10%	
- 100 + 200 mesh	approx. 15%	
- 200 mesh	approx. 27%	

With this coke mixture and 20% of its weight of pitch, the following additives were incorporated into the anode material:-

MATERIAL OF CONSTRUCTION : "COMSTEEL" R4

SCALE : FULL SIZE

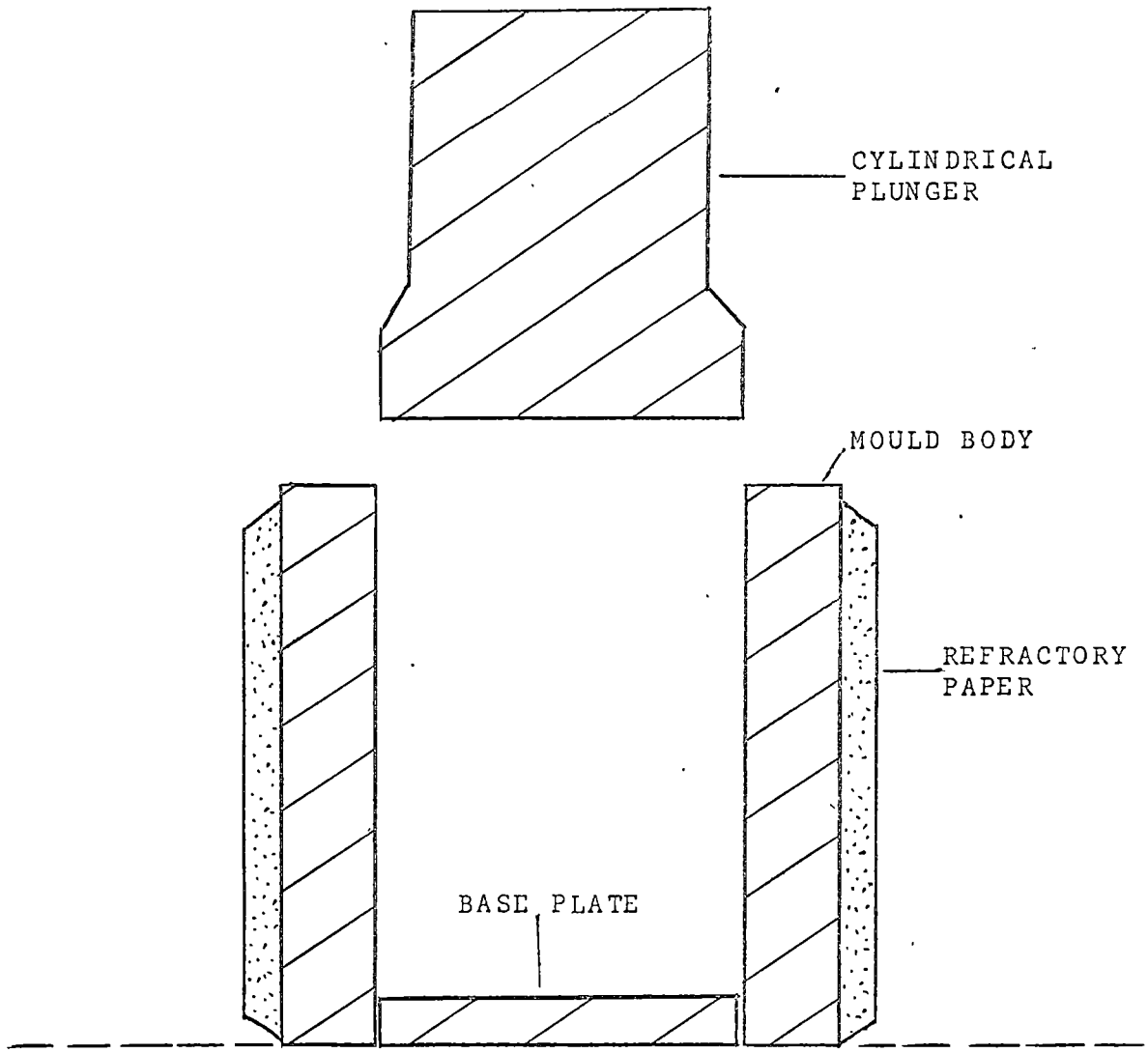

FIGURE 1. ANODE PRESSING MOULD - ELEVATION.

1%, 2% and 5% Al_2O_3

1% and 2% CaF_2

2% each of LiF, AlF_3, Na_3AlF_6, Li_2CO_3, Na_2CO_3 and $CaCO_3$, resulting in twelve separate types of anode (including a blank).

The percentages are expressed on the basis of the amount of petroleum coke in any given anode mixture. Details of the additives used are as follows:-

Al_2O_3 - Normal production material, sieved to -100 mesh B.S.S., digested with 1:1 HCl at the boiling point, washed, dried.

Fe_2O_3 = 0.005%, SiO_2 = 0.014%, Na_2O = 0.015%

CaF_2 - Industrial grade: CaF_2 = 97.6%, SiO_2 = 0.64%

Fe_2O_3 = 0.06%

LiF - Reagent grade.

AlF_3 - Prepared from super-purity aluminium and 50% analytical grade HF.

Al = 34.5%, Fe_2O_3 = 0.11%

Na_3AlF_6 Synthetic cryolite, selected materials.

Na = 32.2%, Fe_2O_3 = 0.015%, SiO_2 = 0.012%,

NaF/AlF_3 ratio : 1.48 (neutrality = 1.50)

(See Appendix A, (vii), for explanatory note)

Na_2CO_3 - Analytical grade.

$CaCO_3$ - Analytical grade.

Li_2CO_3 — Prepared from reagent grade lithium chloride and ammonium carbonate by precipitation.

In addition to the above anode types, a further range of anodes was prepared in which the amount of additive ranged from 10% to approximately 50% of the coke plus additive portion of the total mixture, as shown in the following table. The additive in these cases consisted of partially-hydrated alumina (ignition loss about 10%) obtained as a by-product of the alumina kiln electrostatic precipitators.

			Mixture L.1	Mixture L.2	Mixture L.3
Weight proportions of anode components.	Petroleum Coke	-4 + 20 ##	540	540	-
		-20 + 48 ##	112	112	280
		-48 + 100 ##	134	134	112
		-100 + 200 ##	208	208	124
		-200 ##	230	100	-
	Al_2O_3 ≠		136	272	554
	Pitch		276	276	300
% Pitch			16.9	22.9	21.9
% Al_2O_3 in Coke + Additive			10.0	19.9	51.8

≠ Al_2O_3 partially-hydrated (see above).

In the above cases, experience showed the need for increased percentages of pitch binder to maintain a coherent block after pressing. Also, the amount of -100 mesh coke was progressively reduced so as to maintain a reasonably similar particle size distribution between the three batches, especially in view of the fine nature of the additive (approx. 80 to 90% -325 #Tyler).

The unbaked anodes, both plain and modified, were baked to remove volatile hydrocarbons. The method involved packing a number of the anodes into large refractory crucibles, covering with a coke-type packing material, and baking in an industrial baking furnace.

The conditions consisted of increasing the sample temperature from ambient to 1000°C over a period of 10-12 days in a pre-heating stage, raising from 1000 to 1175°C in 48 hours, and finally cooling to ambient temperature over a further 14 day period.

The samples used in the whole of this work were baked in the above manner under typical plant conditions.

(ii) Contact Angle Measurements

The measurement of the extent of physical contact between the baked anode surface and the molten cryolite flux was made using a method based on that used by Vajna (6). The principle consists of photo-

graphing the flux-carbon interface whilst the sample is contained in a horizontal tube furnace at about 1,000°C.

In this work, the equipment consisted of that shown in Figures 2 and 3. The furnace comprised a 3-5/8in inside diameter tube fabricated from inconel sheet, heated over a length of 26in by a concentric heavy-gauge nichrome element operating on a maximum of 39V. The tube was fitted with cooling jackets near each end, and provision was made for a range of gaseous atmospheres to be used in the interior.

The ends of the furnace tube were fitted with circular graphite plates 6in diameter and 1in thick, one of which was fitted with a simple metal stopcock as a gas outlet. The viewing end-plate contained a centrally-located calcium fluoride window 25mm in diameter through which the melting and contact phenomena could be observed.

The anode sample under study was machined into a cylinder 2in diameter and 1in high and placed on a stainless steel platform in the centre of the furnace tube, so that the upper surface of the anode, on which a small fused bead of flux rested, was co-linear with the horizontal diameter of the furnace.

The whole apparatus, when completely assembled in

its insulating body and mounted on supporting brickwork, had an overall length of 37in, and a height of 18in.

Anode samples investigated were selected from those listed in the previous section, along with graphite; flux materials comprised pure cryolite, cryolite with 5% by weight of alumina, and a material composed of 85% (by weight) of cryolite, 7% calcium fluoride, 5% alumina and 3% aluminium fluoride. This latter sample was prepared to give a flux approximately in composition to that encountered in a Hall reduction furnace. All flux samples were prepared by fusing suitable amounts of the components in a small covered graphite crucible at 1050°C, stirring with a graphite rod to mix, and allowing to cool to room temperature. The resulting solid was then broken into "chips" of a suitable size for use in contact angle work.

Because of the dependence of interfacial contact on the surrounding atmosphere (6), the following gases were variously used in this phase of work:-

Dry argon

Dry carbon dioxide

Dry carbon dioxide 70% v/v - carbon monoxide 30% v/v

The last named mixture contains approximately the same

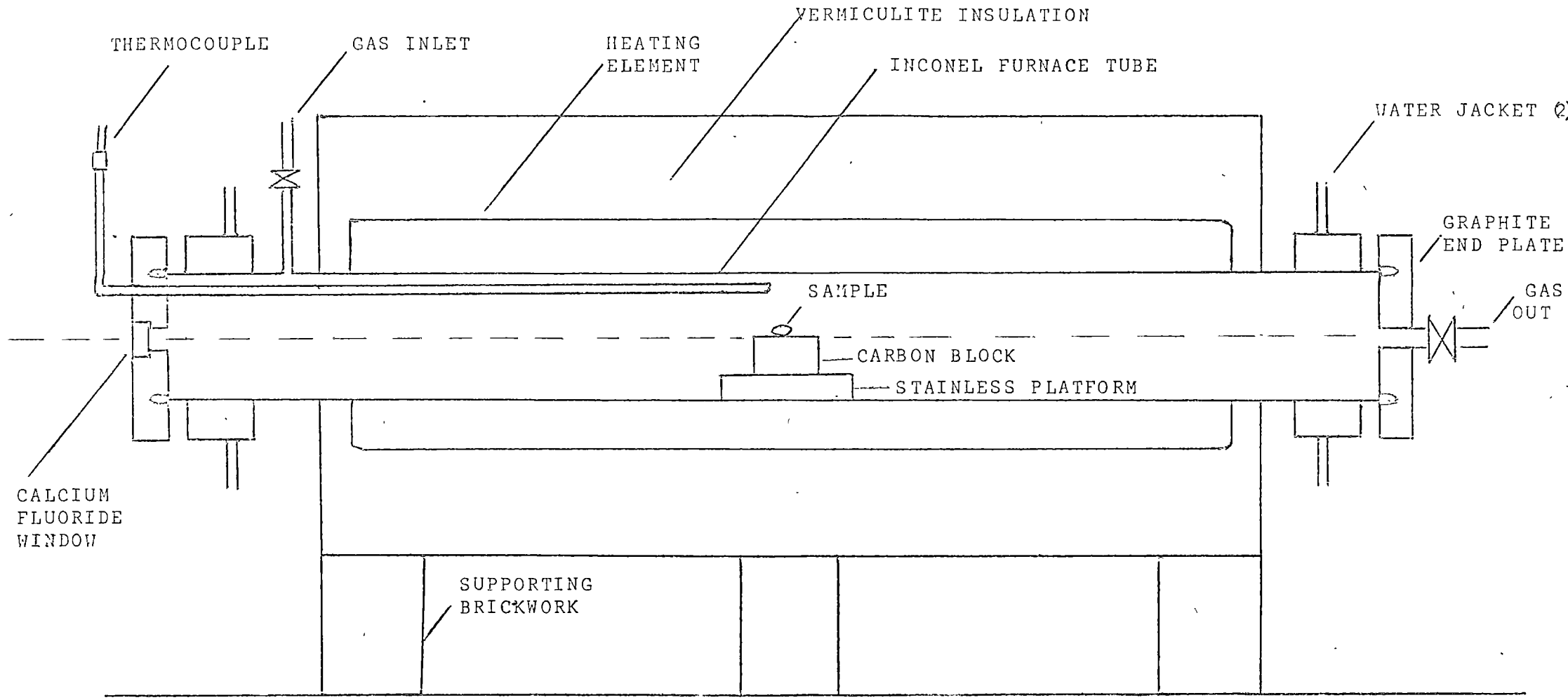

FIGURE 2.

HORIZONTAL TUBE FURNACE FOR CONTACT ANGLE MEASUREMENTS - SIDE ELEVATION

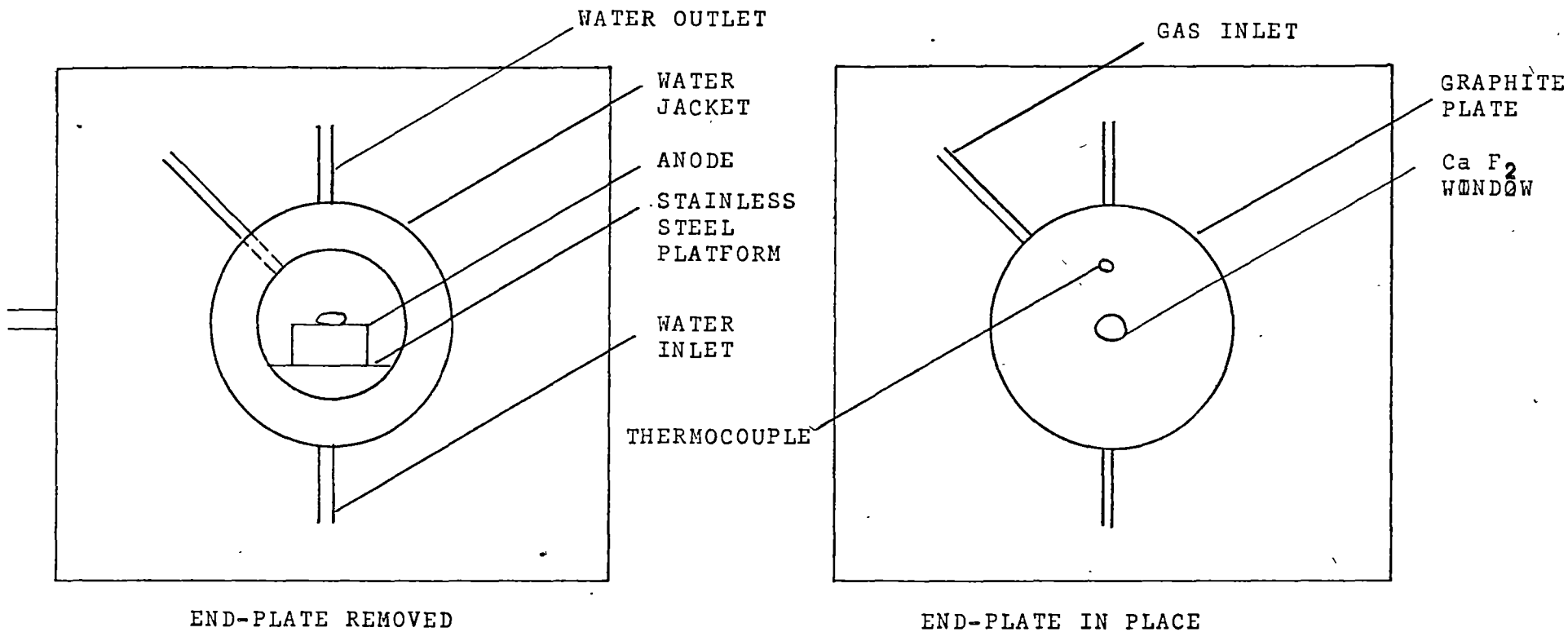

Figure 3

HORIZONTAL TUBE FURNACE FOR CONTACT ANGLE MEASUREMENTS - END ELEVATION

ratio of oxides of carbon as occurs in the anode environment of an industrial reduction furnace.

All gases were delivered to the apparatus from cylinders, after drying in a train of towers containing concentrated sulphuric acid, and lump calcium chloride, at approximately 250 ml/min.

When the anode and flux samples had been placed in the furnace, cold tap-water was circulated through the cooling jackets at approximately 1.0 l/min, and the centre of the furnace heated by means of the nichrome element provided. Temperature indication and control was provided by a "Cambridge" indicator/controller, operating through a "Pyrotenax" chromel-alumel thermocouple.

The phenomena of melting, contact angle and adhesion, were recorded photographically. A tripod-mounted 35 mm camera, fitted with extension bellows and a 135 mm focal length lens was used, employing black-and-white panchromatic film. Exposures of $\frac{1}{2}$s at an f/8 aperture with a film of 125 A.S.A. speed rating gave the most satisfactory results at sample temperatures of 975 - 1000°C. No extra illumination other than that provided by the sample was needed.

The photographic records were made from the time the flux began to melt until a stable molten bead was

obtained on the carbon surface. The number and type of photographs depended on the nature of the individual samples as melting progressed.

From this point on, conventional darkroom techniques were used to obtain enlarged images of the observed phenomena. From the prints, geometric measurements of contact angles could be made, and comparisons between anodes of various compositions could be measured.

(c) Results:

(i) Anode Preparation and Properties.

Using the method outlined, no major problems were encountered in the pressing and baking of the anode samples. Typical specimens are shown in Figure 4, both in the baked condition and prepared for contact angle measurements. The unbaked blocks showed no indication of the presence of any additive materials. The pressing conditions are represented by the following average figures for five separate mixtures:-

Mix No.	Average Pressure. (lb/sq in)	Additive	No. of blocks in mix.
1	5671	Nil	14
2	5650	1%Al_2O_3	26
3	5591	5%Al_2O_3	27
4	5633	1%CaF_2	27
5	5592	22%Al_2O_3	26

The high proportion of alumina in Mix No. 5 resulted from the replacement of half of the 200 mesh fraction of petroleum coke with alumina. The proportion of pitch was unchanged. However, the condition of these blocks after baking was generally unsatisfactory, being of a crumbly texture.

The incorporation of high percentages of additives such as alumina (being the only practical additive at

high levels, e.g., 50%) could only be achieved using higher amounts of pitch binder, as referred to in a previous section, if a satisfactory baked block was to be obtained.

In the instances where the additive material consisted of a compound with a tendency to decompose or partly volatilise at the baking conditions, no evidence was obtained of surface irregularities or internal stresses in the baked anodes. This applied to those anodes containing cryolite, aluminium fluoride, lithium fluoride, calcium, lithium, and sodium carbonates, and partially-hydrated alumina, all additives with a tendency to alter in form at the temperatures used in baking.

The stability of this type of block is further in evidence by the results of ash determinations on samples of the baked anodes, as shown below. The samples were ashed to constant weight at 700°C in an electric muffle furnace allowing a free access of air to the material.

Additive (weight %)	% Ash (700°C, constant weight)
None	1.2
None	1.3
2% Al_2O_3	2.1
5% Al_2O_3	6.9

2% LiF	2.9
2% Li_2CO_3	2.6
2% CaF_2	3.6
2% $CaCO_3$	3.4
2% AlF_3	2.3

In the case of anodes containing additives which would melt at the baking temperatures, one would expect a considerable loss of material during baking, due to either seepage or volatilization, with a correspondingly lower ash content. An explanation which is put forward is that with a low percentage of additive evenly dispersed throughout the samples, the surface-active amorphous carbon particles have retained the molten salt, probably by adsorption onto solid anode material.

Baking conditions representative of those used in the preparation of these anodes are shown in the following table:-

Time (h)	Temperature (°C)
0	975
4	990
8	1000
12	1015
16	1040
20	1055
24	1075

28	1100
32	1120
36	1150
40	1170
44	1175
48	1185
52	1190

A 14-day pre-heating period and a similar cooling time were associated with the above baking cycle.

The overall condition of the baked blocks was that of a semi-porous sample, which could be machined and drilled without physical deterioration for the required purposes (See Fig. 4).

(ii) Contact Angle Furnace Operation

The furnace used for contact angle studies was operated from a low-voltage (39V max.), 5 KVA transformer, and the times taken to reach 1000°C from ambient temperature under several conditions were as shown:-

Input voltage	Watts	Time to 1000°C
33	2750	200 min
36	3275	140 min
39	3820	115 min

The times taken to reach 1000°C in the centre of the furnace were obtained with argon flow-rate of 200 ml/min and a water flow-rate of 1 l/min.

A certain amount of power was lost from the system in the water-cooled end-jackets. The following table lists the details of water flow and temperatures, and corresponding loss of power in this way. Losses due to radiation from the furnace end plates and gas stream were not determined; the temperature of the outer surface of these plates was of the order of 250°C when the furnace interior was at 1000°C.

Centre of furnace (°C)	Water flow-rate	Water temperature In	Out	Power loss
545	1.03 l/min	10.2°C	15.0°C	346W
800	1.05 l/min	10.8°C	19.0°C	600W
850	1.03 l/min	10.8°C	20.9°C	720W

To determine the temperature distribution within the heated zone of the furnace at normal operating temperatures a traverse was performed along the entire heated length. For this purpose, the apparatus was operated at a controlled temperature of 1,000°C, with no sample, but normal argon and water flows.

The controlling thermocouple was placed midway along the furnace tube, and a second similar thermocouple inserted from the other end such that it could be moved stepwise along the apparatus to measure the

temperature gradient. At each point the on-off cycle was measured potentiometrically several times, and compared with a similar measurement on the controlling thermocouple. The results are shown in the following table and graph.

Distance along heated length. (inches)	Temperature (°C) during on-off cycle. Maximum	Minimum
0	759	753
1	822	813
2	873	862
3	910	897
4	940	927
5	964	948
6	984	968
7	999	983
8	1011	995
9	1019	1003
10	1022	1007
11	1020	1006
12	1019	1005
13	1013	1001
14	1005	995
15	993	980
16	979	966
17	958	946

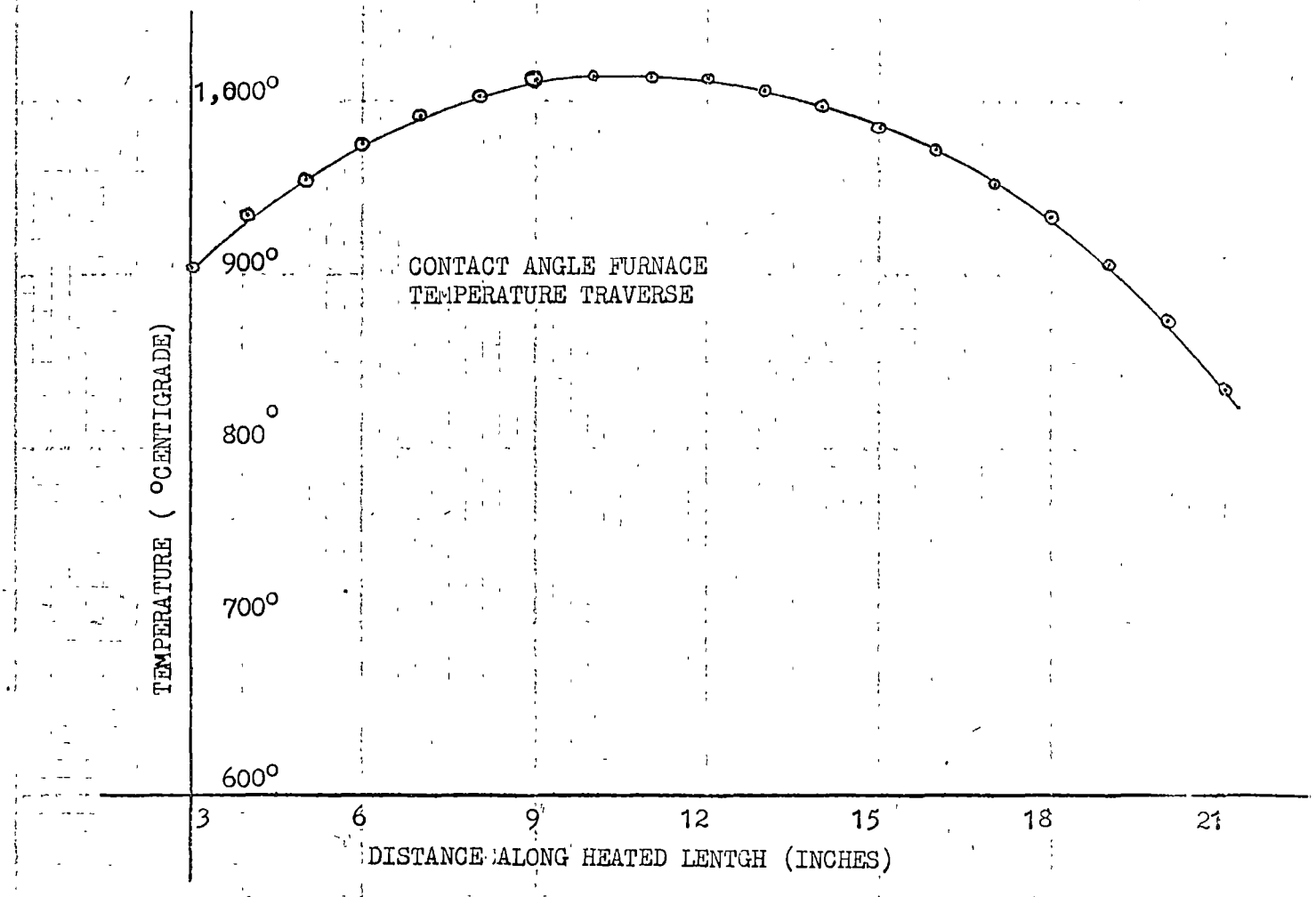
CONTACT ANGLE FURNACE
TEMPERATURE TRAVERSE
TEMPERATURE (°CENTIGRADE)
1,600°
900°
800°
700°
600°
3
6
9
12
15
18
21
DISTANCE ALONG HEATED LENTGH (INCHES)

18	938	925
19	914	901
20	882	970
21	838	829
22	779	772
23	712	708
24	603	601

(iii) Observation of Melting Phenomena

Practically all of the experimental runs in this section of work followed patterns of a similar type, but varying in degree. The general pattern observed consisted of the sequence: melting-adhesion-absorption. Each of these stages depended for its exact behaviour on the nature of the anode and its additive, the flux composition, and the surrounding atmosphere in the furnace.

Typical examples of each stage are shown in Fig. 5 - 7; these have been selected to illustrate the above mentioned phenomena. Particular features which have been observed throughout the contact angle studies include:-

1) Melting of fluxes in an atmosphere of argon resulted in practically no adhesion to the carbon sample. This was the case in most instances, and the presence

of a range of additives had almost no effect on the extent of adhesion of cryolitic fluxes.

The exceptions have been anodes containing 10-25% alumina (as kiln dust) in contact with a flux of cryolite/5% Al_2O_3. These are shown in Figures 8 and 9 and can be compared with Figure 10, showing an unmodified anode and a normal flux sample.

Thus, the technique of Vajna (6) has been extended to include amorphous carbon samples which have been modified by additives, and also varying flux compositions. However, the observation that no type of carbon is wetted by cryolite in an atmosphere of argon should now be modified to include the behaviour of the anodes referred to in the previous paragraph.

2) The use of an atmosphere of carbon dioxide in the apparatus brought about an increased tendency for the beads of molten flux to adhere to the carbon surfaces.

Carbon dioxide represents an increase in the oxidizing power of the atmosphere employed, and a comparison between this gas and argon was readily made by melting the flux under argon and changing to a stream of carbon dioxide, at the same time

continuously observing and recording the alteration in interfacial behaviour.

Of the additives tested under carbon dioxide, the most adhesive beads, as observed from the profile of the molten sample on the carbon, were obtained with anode additives of 10% alumina, 2% lithium fluoride, 2% lithium carbonate, or 2% cryolite. The composition of the flux, within practical limits, did not significantly affect the overall results.

3) Earlier reference has been made to the use of a 70 volume percent carbon dioxide - 30 volume percent carbon monoxide atmosphere in the contact angle furnace because of its similarity to the ratio of oxides of carbon found in the anode vicinity in an industrial furnace. It was not expected that any appreciable difference would be observed when compared with an all-CO_2 atmosphere. This was generally confirmed experimentally.

In reviewing the results obtained, it can be seen from the attached illustrations (Fig. 11 - 14) that lithium carbonate, lithium fluoride, calcium fluoride, and calcium carbonate, all at the 2% level, were effective in promoting interfacial contact under conditions approaching those found in practice, whereas 2% AlF_3 in the anode showed no improvement in adhesion (Fig. 15).

Of particular significance is the result obtained when an unmodified block was used with a cryolite/5% alumina flux. The illustration (Fig. 16) shows a total lack of contact between the two phases. The cool bead was readily removed, leaving no trace of the flux adhering to the block. A very similar result was obtained using a flux of normal composition as found in practice.

4) The admission of air, at the same flow-rate as the other gases, caused a rapid lowering of the contact angle, accompanied by an absorption of the flux into the block. This took place within ten to fifteen minutes. It appeared to be governed by the air flow-rate, and the process could be arrested, but not reversed, by the re-admission of CO_2 to the exclusion of the air stream.

The only instance where the admission of air did not cause flux absorption by the carbon was in the case of a graphite block. This observation is in keeping with the non-wetting of graphite by cryolite under all atmospheres (6).

5) One feature of the behaviour of cryolite fluxes under these conditions does not appear to have been recorded. it concerns the "physical stability" of the system as a function of the oxidizing nature of the surrounding atmosphere.

When using argon as the furnace gas, the molten bead of flux remains stable and quiescent on the carbon surface. As mentioned earlier, the chemical inertness and interfacial dissimilarity are doubtless responsible for this condition.

However, when air is admitted to the furnace, the system loses its stability, and a bubbling action commences within the molten flux. These bubbles grow within the flux, and finally break through the upper surface of the bead, which then collapses to its original configuration. At the same time, absorption of the flux into the carbon continues. This alternating rise-and-fall cycle of the molten flux continues until the bead is absorbed into the carbon. Alternatively, the phenomenon could be halted by replacing the air stream with a stream of argon.

The cause of this bubbling action illustrated in Figures 17 and 18 was not determined. The evidence suggests that it is caused by the presence of air, and the suggestion is put forward that the bubbles consist of oxides of carbon which form below the flux and gradually come to the surface.

6) The tendency for cryolite melts to fume strongly is one which introduces experimental difficulties when working with such materials. During the course of

this work, the tendency of the flux samples to generate such fumes created problems in photographing some of the runs. The most satisfactory solution proved to be the application of a gentle suction to the outlet end of the furnace tube at a rate matching the flow-rate of the incoming atmosphere. The gases were then led through a water cooled condenser system and vented to outside.

(iv) Contact Angle Measurements

Although contact angle studies at high temperatures is not a new field, the attention which has been given to the cryolite-carbon systems from a quantitative aspect seems to be limited. Vajna (6) has made a study of this system, but in the work referred to gives no quantitative measurement of the equilibrium contact angle which may be used as a reference value for the present work. He states that "when the gas is N_2, CO, CO_2, HF and CF_4, the drop does not moisten the carbon and the angle θ remains obtuse ..... on amorphous carbon ..... for all types of solutions."

Belyaev (6a) quotes a contact angle of 127° for cryolite on carbon at $1005^{\circ}C$, but the data he presents shows the influence of flux composition on contact angle, and not a variation in carbon composition, as has been studied in this work. Similar results have

been reported by Matiasovsky et al. (6b).

In the present work, an angle of 180° is defined as that obtained between solid and liquid phases in contact when the former is not wetted by the latter. Conversely, when wetting is complete, the contact angle is zero.

The measurement of contact angles in this work has been made geometrically, using the profile obtained by photographing the molten drop on the carbon anode.

The factor limiting the accuracy of this method lies in the drawing of the tangent to the liquid surface at its point of contact with the carbon. The reproducibility of this tangent was determined by making a series of twenty identical prints of a typical profile. On each of these, a tangent was drawn and the contact angle measured. By this method, a mean value of 136° was obtained for the sample chosen, and a standard deviation of $\pm 2^{\circ}$ calculated.

In all results tabulated below, the contact angle is the mean of the two angles on either side of the profile of the molten flux sample.

Illustrations representative of a number of contact profiles are shown, along with examples of varying adhesion between flux and carbon. (Fig. 8 - 16; 19 - 28)

Table 1: Contact Angles in Argon Atmosphere.

Additive in Anode	Flux Composition	Contact Angle θ	Temp. (°C)	Fig. No.
Nil	Cryolite	148°	1,000	
Nil	Cryolite - 5% Al_2O_3	137°	996	19
Nil	85-7-5-3 ≠	124°	1,003	10
1% Al_2O_3	Cryolite	131°	1,012	
"	"	137°	1,020	
"	Cryolite - 5% Al_2O_3	135°	1,002	
5% Al_2O_3	Cryolite	137°	985	
"	Cryolite - 5% Al_2O_3	133°	999	20
"	85-7-5-3 ≠	132°	1,002	
1% CaF_2	" ≠	133°	1,001	
"	Cryolite	137°	1,022	
"	Cryolite - 5% Al_2O_3	128°	1,000	
2% Li_2CO_3	85-7-5-3 ≠	136°	1,027	21
"	Cryolite - 5% Al_2O_3	133°	1,036	
2% Cryolite	" "	118°	1,030	
2% LiF	Cryolite	118°	1,019	
All Graphite	"	129°	1,000	
" "	85-7-5-3 ≠	136°	1,000	
10% Al_2O_3 +	Cryolite - 5% Al_2O_3	Acute	1,000	8
25% Al_2O_3 +	" "	"	980	9

Table 2: Contact Angles in CO_2 Atmosphere.

Additive in Anode	Flux Composition	Contact Angle θ	Temp. (°C)	Fig. No.
All Graphite	Cryolite	125°	1,040	
Nil	"	115°	1,039	
1% Al_2O_3	"	79°	1,048	
(θ = 121° in argon before admission of CO_2.)				
1% Al_2O_3	Cryolite - 5% Al_2O_3	88°	Not noted	23
5% Al_2O_3	85-7-5-3 ≠	93°	1,013	
2% LiF	Cryolite	102°	1,026	
2% Cryolite	Cryolite - 5% Al_2O_3	80°	1,050	22
(θ decreases rapidly with time.)				
10% Al_2O_3 +	Cryolite - 5% Al_2O_3	76°	1,000	
1% CaF_2	85-7-5-3 ≠	94°	1,004	24

≠ The figures 85-7-5-3 refer to a flux containing 85% cryolite, 7% calcium fluoride, 5% alumina, and 3% aluminium fluoride, pre-melted prior to use.

\+ Alumina present in amounts over 5% has been added as recovered calciner kiln dust.

Table 3: Contact Angles in 70% CO_2 - 30% CO Atmosphere.

Additive in Anode	Flux Composition	Contact Angle θ	Temp. (°C)	Fig. No.
Nil	Cryolite - 5% Al_2O_3	125°	1,029	16
2% CaF_2	" "	Very acute	1,036	13
"	Normal Flux ≠	100°	990	
2% $CaCO_3$	" " ≠	77°	990	
"	Cryolite - 5% Al_2O_3	99°	1,028	14
2% Na_2CO_3	" "	92°	1,016	
2% AlF_3	" "	118°	1,020	15
2% LiF	" "	111°	1,024	12
2% Li_2CO_3	" "	Acute	1,024	11

Table 4: Extent of Physical Adhesion of Flux to Anode Samples.

Atmosphere	Additive in Anode	Flux Composition	Extent of Adhesion	Fig. No.
Argon	Nil 1% Al_2O_3 5% Al_2O_3 1% CaF_2 2% LiF 2% Cryolite	Cryolite only	No apparent evidence of adhesion of flux to anode.	
Argon	Nil 1% Al_2O_3 5% Al_2O_3 1% CaF_2 2% Cryolite	Cryolite - 5% Al_2O_3	No apparent evidence of adhesion.	

Table 4 cont: Extent of Physical Adhesion of Flux to Anode Samples.

Atmosphere	Additive in Anode	Flux Composition	Extent of Adhesion	Fig. No.
Argon	Nil 1% Al_2O_3 5% Al_2O_3 1% CaF_2	85-7-5-3	No apparent evidence of adhesion.	
Argon	10% Al_2O_3 25% Al_2O_3	Cryolite - 5% Al_2O_3	Good adhesion.	29
CO_2	Nil 1% Al_2O_3 5% Al_2O_3 2% Cryolite	Cryolite only	No apparent adhesion.	
CO_2	1% Al_2O_3 5% Al_2O_3 1% CaF_2	85-7-5-3	No apparent adhesion.	
CO_2	2% LiF	Cryolite	Moderate adhesion.	
CO_2	1% Al_2O_3 2% Li_2CO_3	Cryolite - 5% Al_2O_3	Moderate adhesion.	
CO_2	2% Li_2CO_3	85-7-5-3	Good adhesion.	
CO_2	2% Cryolite 10% Al_2O_3	Cryolite - 5% Al_2O_3	Good adhesion	28
70% CO_2 -30% CO	Nil 2% AlF_3	Cryolite - 5% Al_2O_3	No apparent adhesion.	

Table 4 Cont.: Extent of Physical Adhesion of Flux to Anode Samples.

Atmosphere	Additive in Anode	Flux Composition	Extent of Adhesion	Fig. No.
70% CO_2 -30% CO	Nil	Normal Flux ≠	No apparent adhesion.	25
70% CO_2 -30% CO	2% $CaCO_3$ 2% Na_2CO_3 2% Al_2O_3	Cryolite - 5% Al_2O_3	Low to moderate adhesion.	
70% CO_2 -30% CO	2% LiF 2% Li_2CO_3 2% CaF_2	Cryolite - 5% Al_2O_3	Good adhesion.	27
70% CO_2 -30% CO	2% CaF_2 2% $CaCO_3$	Normal Flux ≠	Good adhesion.	26

≠ Normal Flux - a standard cryolite-based electrolyte, with a NaF/AlF_3 ratio of 1.40.

(d) Discussion:

From the above results, it is apparent that when an argon atmosphere is used, the contact angle of the flux bead on the carbon surface is generally of the order of 135°. Allowing for the accuracy of the geometric measurements and the fact that the porous surface cannot be reproduced exactly from one measurement to the next, it is concluded that practical deviations from the cryolite composition do not significantly effect the contact angle between the two phases. The same comment can be made concerning the amount and type of additive incorporated into the carbon.

In assessing the influence of additives on adhesion and contact angle, a relatively large effect has been sought from a small percentage of additive. In particular, a change from an obtuse to an acute angle has been considered strong evidence in this work, of increased interfacial adhesion.

The effect of carbon dioxide atmosphere on contact angle can be measured on a semi-quantitative basis by comparing results from corresponding conditions in Tables 1 and 2.

In addition to the changes in contact angle brought about by varying the type of anode and surrounding atmosphere, the extent of adhesion between the contact area of flux and anode is significant. When adhesion

(d) Discussion:

From the above results, it is apparent that when an argon atmosphere is used, the contact angle of the flux bead on the carbon surface is generally of the order of 135°. Allowing for the accuracy of the geometric measurements and the fact that the porous surface cannot be reproduced exactly from one measurement to the next, it is concluded that practical deviations from the cryolite composition do not significantly effect the contact angle between the two phases. The same comment can be made concerning the amount and type of additive incorporated into the carbon.

In assessing the influence of additives on adhesion and contact angle, a relatively large effect has been sought from a small percentage of additive. In particular, a change from an obtuse to an acute angle has been considered strong evidence in this work, of increased interfacial adhesion.

The effect of carbon dioxide atmosphere on contact angle can be measured on a semi-quantitative basis by comparing results from corresponding conditions in Tables 1 and 2.

In addition to the changes in contact angle brought about by varying the type of anode and surrounding atmosphere, the extent of adhesion between the contact area of flux and anode is significant. When adhesion

of the flux to the anode surface is pronounced, as observed from the difficulty of their separation when cool, this can be taken as additional evidence of affinity between the surfaces (see Table 4).

If this affinity extends over a large area in an industrial furnace, then considerable improvements in operating conditions can be predicted. If the mutual affinity of the flux and carbon surfaces is sufficient to overcome the tendency for bubbles of anode gases to accumulate under the anode during electrolysis, speedier removal of the main anode product, CO_2, will be expected to result, leading to a saving in carbon consumption.

Summarizing the data from Tables 1 - 4 , above, it is suggested that the most significant results occur in atmospheres of CO_2, and mixed CO_2 - CO, which are the types of gaseous environments encountered in a production furnace. A marked drop in contact angle and an increase in adhesion occur when a plain anode is replaced by one which has been modified.

In some cases, the extent of wetting is sufficient to render the geometric method unsuitable. In such cases, a visual and qualitative estimation of the effect of the anode additive, in terms of extent of adhesion, had to be made.

Industrially, the results suggest that the most

practical additives to include in anode blocks would be calcium fluoride, lithium or calcium carbonates, alumina, and lithium fluoride.

Finally, the lack of adhesion of melts in CO_2 atmospheres, and the very existence of the anode overvoltage, can together be taken as evidence that CO_2, and not oxygen, is the anode product at practical current densities. This interpretation is contrary to the suggestion (6) that "it is oxygen which is first released on the carbon of the anode; then we have the oxidation of carbon into CO and CO_2". If oxygen were released elementally at the anode, then immediate adhesion of flux to carbon would be expected to occur, and any overvoltage due to poor wettability would virtually disappear.

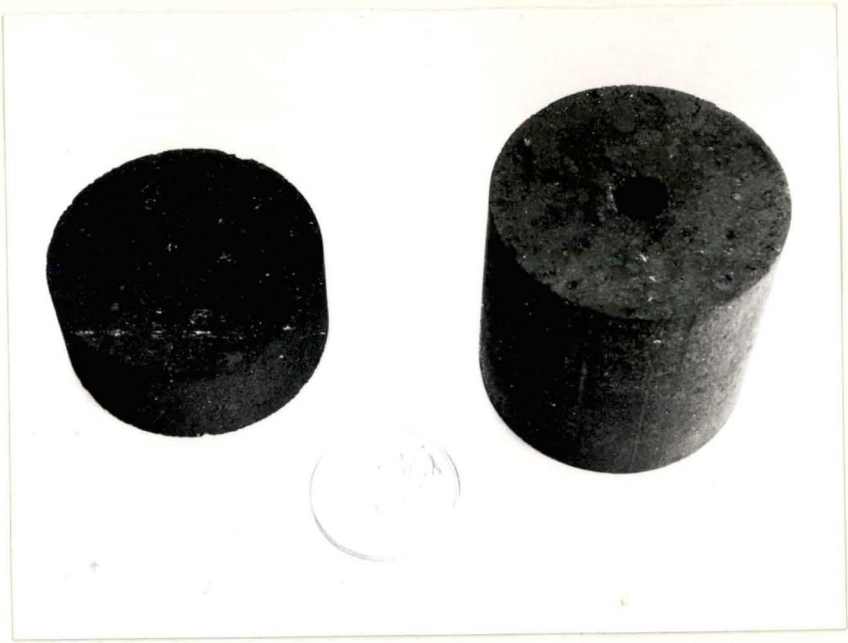

Figure 4: Baked anode specimens; (l) for contact angle measurements, (r) for use in laboratory reduction cell.

Figure 5: Showing early stages of melting flux sample on carbon anode.

Figure 6: Completely molten flux on carbon anode - a typical observation of sample profile.

Figure 7: Absorption of flux into carbon occurring in presence of air.

Figure 8: Showing adhesion of Cryolite - 5% Al_2O_3 flux to anode containing 10% Al_2O_3, under argon atmosphere.

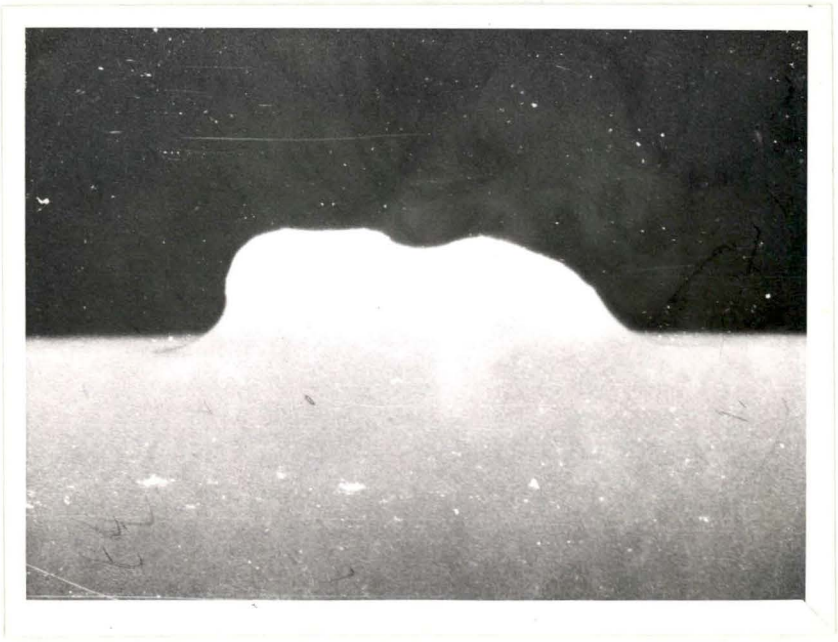

Figure 9: Showing adhesion of Cryolite - 5% Al_2O_3 flux to anode containing 25% Al_2O_3, under argon atmosphere.

Figure 10: Normal flux on unmodified carbon anode, under argon atmosphere.
Note lack of adhesion (cf. Fig. 8 and 9)

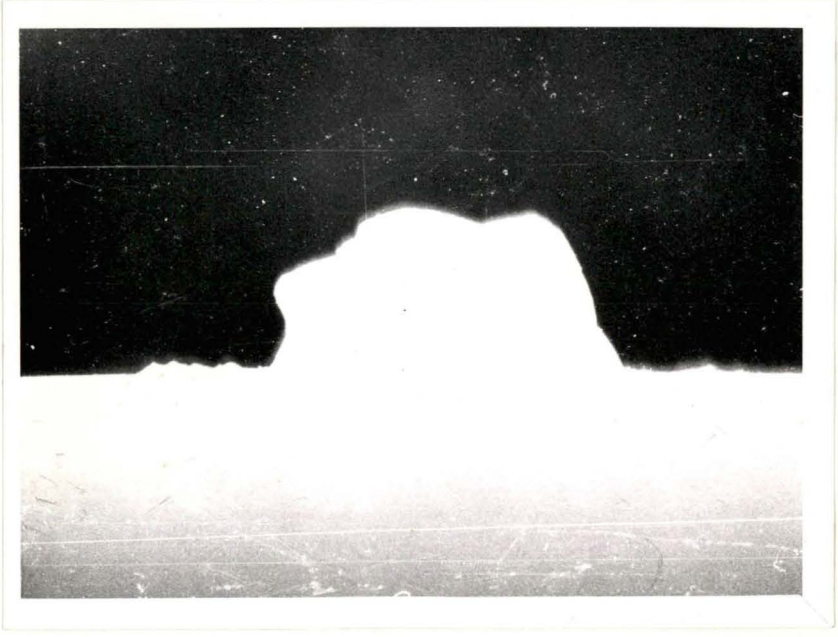

Figure 11: Showing adhesion of Cryolite - 5% Al_2O_3 flux to anode containing 2% Li_2CO_3, under CO_2 - CO atmosphere.

Figure 12: Showing adhesion of Cryolite - 5% Al_2O_3 flux to anode containing 2% LiF, under CO_2 - CO atmosphere.

Figure 13: Showing adhesion of Cryolite - 5% Al_2O_3 flux to anode containing 2% CaF_2, under CO_2 - CO atmosphere.

Figure 14: Showing adhesion of Cryolite - 5% Al_2O_3 flux to anode containing 2% $CaCO_3$, under CO_2 - CO atmosphere.

Figure 15: Showing molten cryolite - 5% Al_2O_3 flux on anode containing 2% AlF_3, under CO_2 - CO atmosphere. Note lack of adhesion.

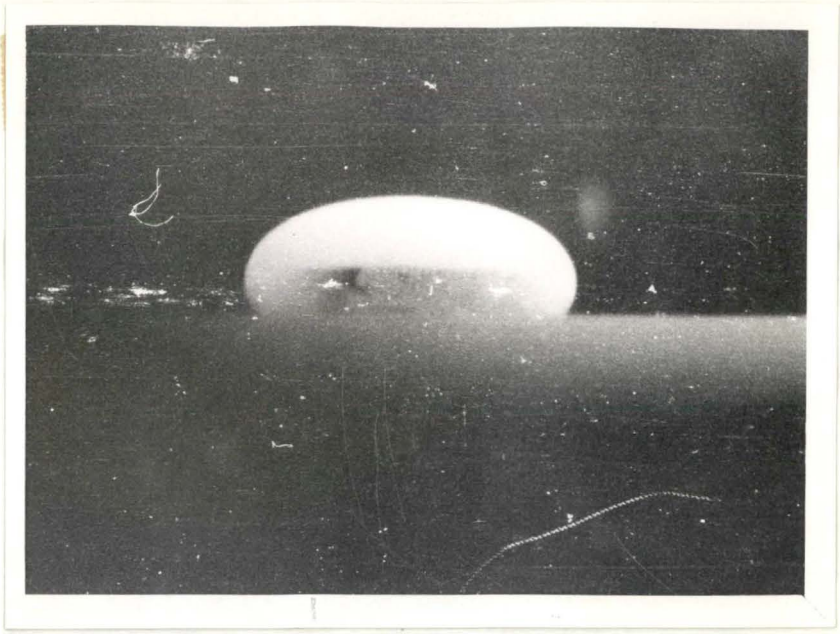

Figure 16: Showing molten Cryolite - 5% Al_2O_3 flux on plain anode, under CO_2 - CO atmosphere; lack of adhesion is again apparent.

Figure 17: Showing bubbling offlux under CO_2 atmosphere.

Figure 18: As for Fig. 17, after collapse of bubble within flux bead.

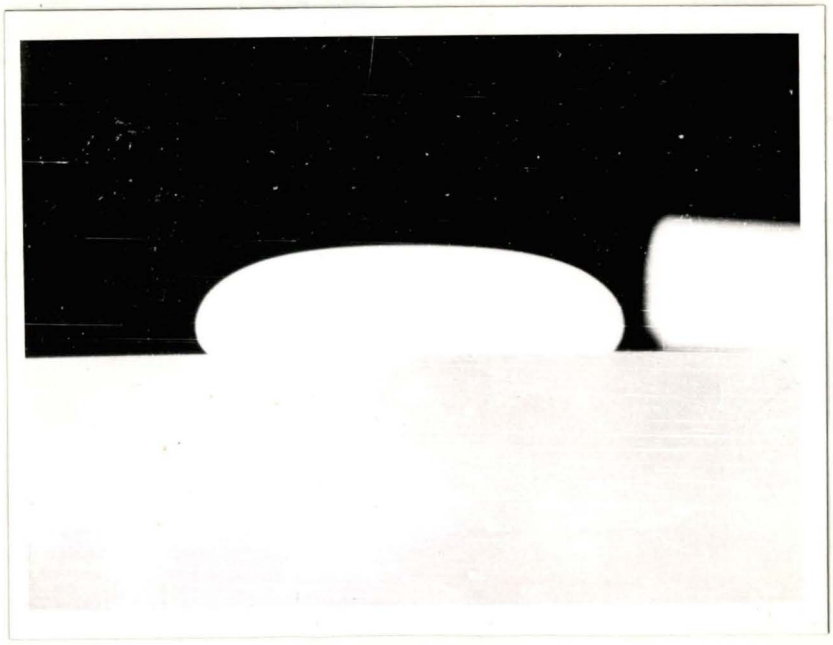

Figure 19: Profile of molten Cryolite - 5% Al_2O_3 flux on plain anode, under argon atmosphere. Contact angle $\simeq 137^{o}$.

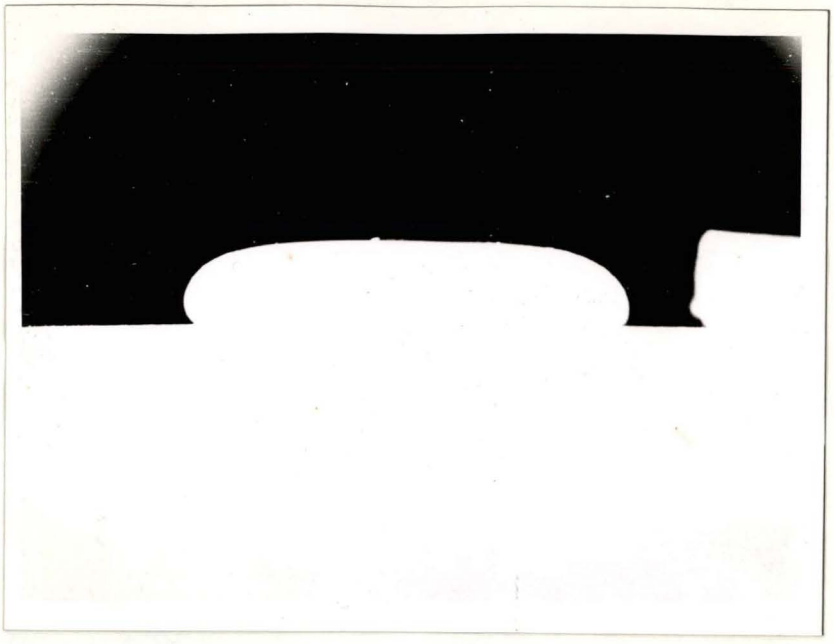

Figure 20: Profile of molten Cryolite - 5% Al_2O_3 flux on anode containing 5% Al_2O_3 under argon atmosphere. Contact angle $\simeq 133^{\circ}$.

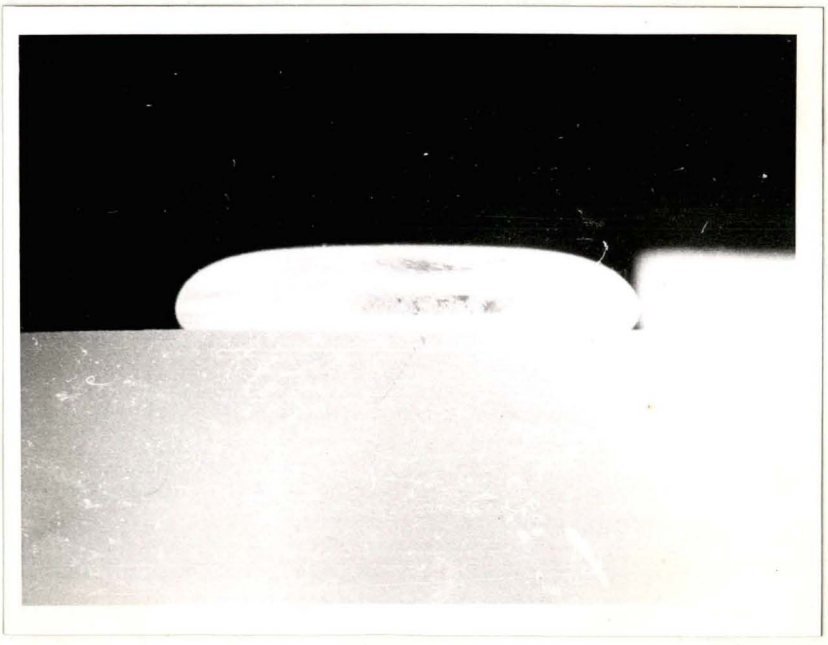

Figure 21: Profile of normal flux on anode containing 2% Li_2CO_3 under argon atmosphere. Contact angle $\simeq 136^{\circ}$.

Figure 22: Profile of Cryolite - 5% Al_2O_3 flux on anode containing 2% cryolite under CO_2 atmosphere. Contact angle $\simeq$ 80°

Figure 23: Profile of Cryolite - 5% Al_2O_3 flux on anode containing 1% Al_2O_3 under CO_2 atmosphere. Contact angle $\simeq$ 88°.

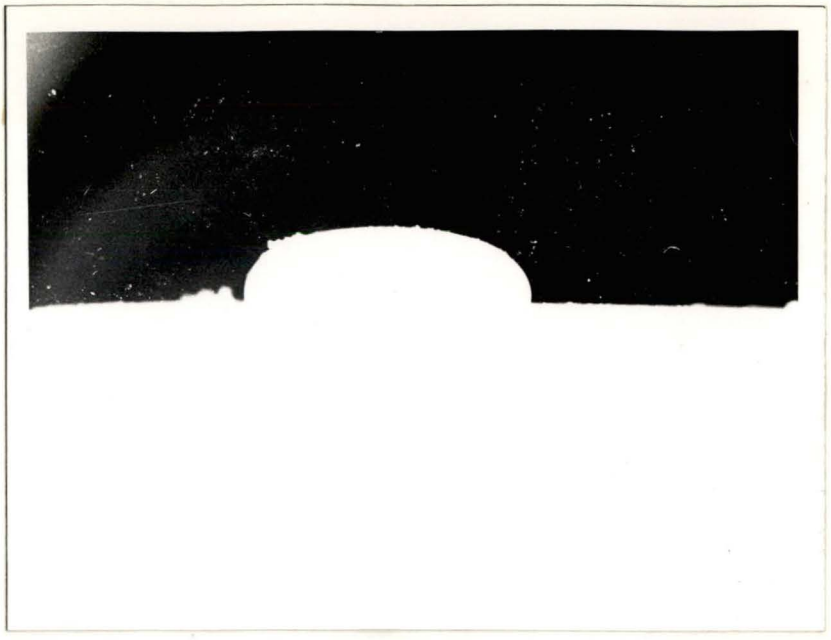

Figure 24: Profile of normal flux on anode containing 1% CaF_2 under CO_2 atmosphere. Contact angle $\simeq 94^{\circ}$.

Figure 25: Showing poor adhesion of normal flux to plain anode after fusion in CO_2 - CO atmosphere.

Figure 26: Showing good adhesion of normal flux to anode containing 2% $CaCO_3$, after fusion in CO_2 - CO atmosphere.

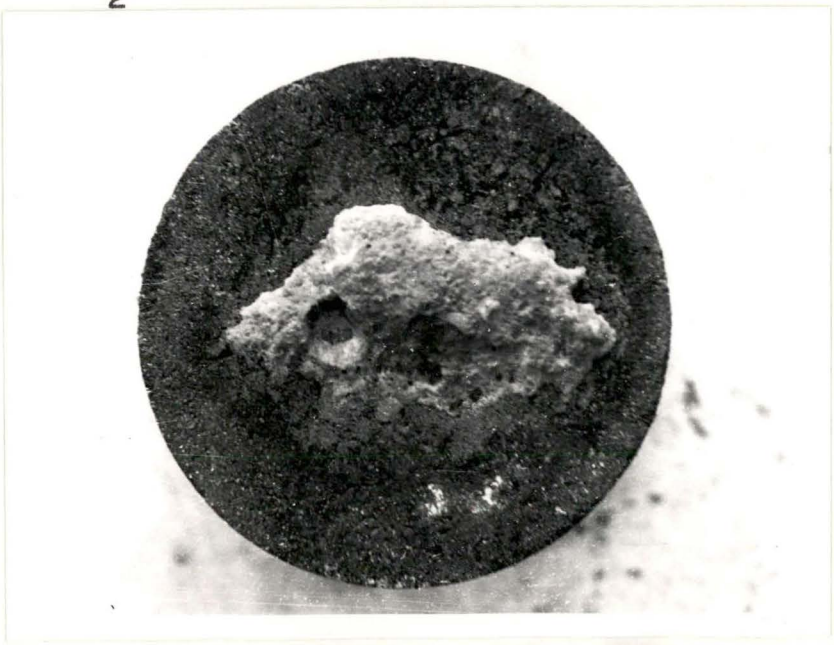

Figure 27: Showing good adhesion and spreading of cryolite - 5% Al_2O_3 on anode containing 2% CaF_2, after fusion in CO_2 - CO atmosphere.

Figure 28: Showing good adhesion and spreading of cryolite - 5% Al_2O_3 flux on anode containing 2% cryolite, after fusion in CO_2 - CO atmosphere.

Figure 29: Showing good adhesion of cryolite - 5% Al_2O_3 flux to anode containing 10% Al_2O_3, after fusion in argon.

PART II : LABORATORY REDUCTION CELL STUDIES

(a) General

Following the investigations into the interfacial phenomena which have been detailed in Part I, wherein the effects of various additives to the carbon on the extent of contact between flux and anode have been studied, a logical step to take was the construction and operation of a laboratory scale reduction cell. By so doing, the performance of all types of anodes prepared for contact angle work could be evaluated under electrolytic conditions. These conditions include for the purpose of this work: operating temperature, flux composition, anode dimensions and type, current and/or current density, total cell voltage, and "overvoltage". The nature of this "overvoltage" is explained in a later section.

From these measurements, it is possible to assess the effects of various additives to the anodes, in terms of total cell voltage, "overvoltage", current density, and current efficiency. It is these operating parameters which help to determine overall furnace performances, especially in as far as they are related to power consumption and carbon consumption per unit weight of metal produced.

As an added advantage, the incorporation of beneficial and compatible additives into the anodes can also provide a practical and continuous method of introducing raw materials into the electrolyte via the anodes, resulting in a more constant flux composition, as well as labour savings.

The extent to which the "wettability" of the carbon anode is improved by the incorporation of the additive materials can also be assessed electrolytically by deliberate production of an anode effect at sufficiently high current densities. The greater the interfacial adhesion, the greater will be the current density required to break this adhesion and cause arc contact, rather than smooth electrolytic conduction. This feature is considered later in this section.

(b) Structure of Cryolitic Melts.

Investigation of the two-component system sodium fluoride - aluminium fluoride began in 1913 with the work of Fedotieff and Iljinski (7). Other workers (8, 9, 10) have also studied this system, and a typical phase diagram, due to Grjotheim (11), is shown overleaf.

Noticeable peaks in the diagram occur at 25 and 50 mole percent AlF_3, corresponding to the compositions of cryolite (Na_3AlF_6) and the compound $NaAlF_4$ respectively.

These compounds, together with chiolite ($Na_5Al_3F_{14}$), are known to contain $AlF_6^{\equiv}$ octahedra, with increasing sharing of fluoride ions between octahedra as the mole fraction of AlF_3 increases.

On melting, cryolite undergoes some dissociation, as indicated by the broadening of the peak in the NaF - AlF_3 phase diagram at 25 mole percent AlF_3. Rolin (12) has suggested that the dissociation of molten cryolite is in agreement with the reaction:-

$$Na_3AlF_6 = 3Na^+ + 3F^- + AlF_3$$

as a value for $\Delta t/m$ of zero is obtained when small amounts of aluminium fluoride are added to molten cryolite. Similar small additions of alumina confirm that AlF_3 is not ionized, and hence there is no ion common to these two compounds.

Additionally, the presence of other aluminium-fluorine species in the melt such as $AlF_5^{=}$ and $AlF_5\text{-}F\text{-}AlF_5^{5-}$, has been postulated by Forland, Storegroven, and Urnes (13), through the reactions:-

$$AlF_6^{\equiv} = AlF_5^{=} + F^-$$

$$\text{or } 2AlF_6^{=} = AlF_5\text{-}F\text{-}AlF_5^{5-} + F^-$$

When dissolved in molten cryolite, alumina ionizes, according to Rolin (12), by one of the following reactions, according to the degree of dilution in the melt:-

$$Al_2O_3 = AlO_2^- + AlO^+$$

$$\text{and } AlO^+ = Al^{+++} + O^{=} \text{ (great dilution)}$$

However, in practical melts in the aluminium industry, one is not dealing with a "neutral" cryolite melt (NaF/AlF_3 weight ratio 1.50), but with a melt to which additional aluminium fluoride has been intentionally added for optimum cell operation. In such solutions, oxy-fluoride anions are considered to be present in one or more forms $(F_2AlO_2AlF_2)^{=}$, $AlO_2F_2^{3-}$, and $AlOF_3^{2-}$ (14,15,16). These are probably formed by the general reaction (Ref. 17):-

$$xAlF_3 + yAlO_2^- = z\left\{Al_{\frac{(x+y)}{2}}\ O_{\frac{2y}{2}}\ F_{\frac{3x}{2}}\right\}^{\frac{y}{z}-}$$

Thus, the ionic structure of these cryolitic melts is a complex one, consisting on the one hand of:

(i) simple cations of the metals present, i.e., Na^{+}, Ca^{++}, (in practical melts), Al^{+++} (in very dilute solutions), and the cation AlO^{+};

(ii) possibly some neutral AlF_3 molecules; and

(iii) the anions F^{-}, AlO_2^{-}, some $O^{=}$, the oxy-fluoro ions referred to above, with small amounts of alumino-fluoride ions.

This complexity of structure is emphasised in a recent review (17a), where reference is made to no less than seventeen ionic species which have been postulated in cryolite-alumina melts.

From these comments, it is considered that the maximum compatability or affinity between melt and anodes will occur when the latter have been impregnated with compounds which, at the operating temperature of the reduction cell, will be in an ionic form, the ions present being those included above.

It is for this reason that fluorides, oxides, and carbonates of sodium calcium, aluminium, and lithium have been used in this work. (Lithium salts are being used in increasing amounts in aluminium smelting.)

Other salts of these metals could presumably be used as anode additives, providing their decomposition at melt temperatures resulted in the formation of ions compatable with the electrolyte.

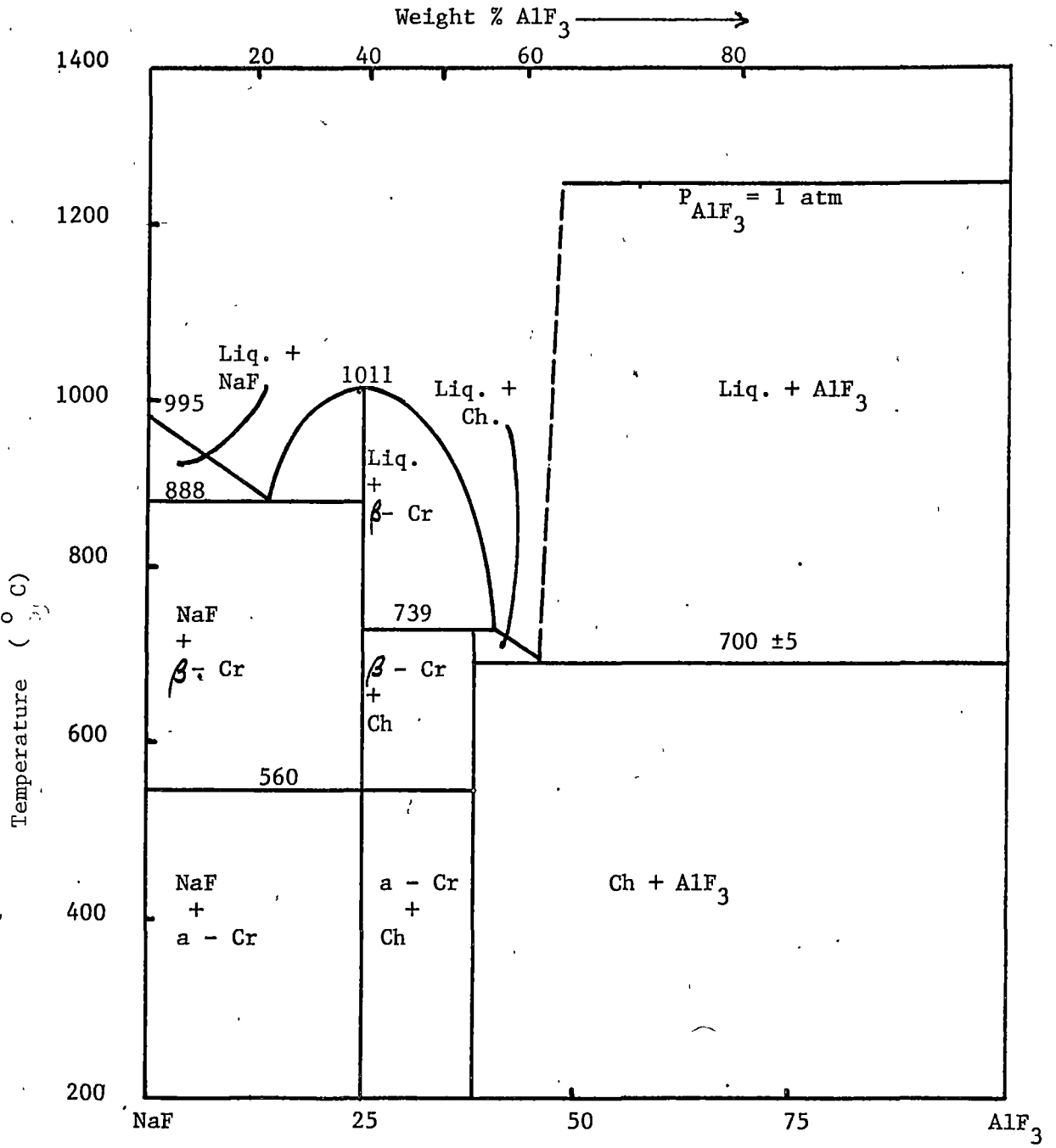

Phase diagram of the NaF – AlF_3 system. (from the work of Grjotheim)

(c) Experimental

(i) Cell Construction

Many designs for laboratory cells for the study of alumina/cryolite electrolysis have been described in the literature (18, 19, 20). Although differing in details, these cells generally follow similar patterns, consisting of a graphite crucible as cathode, placed securely in a suitable cylindrical metal container, with a powdered coke packing to ensure good electrical contact. Both inconel and stainless steel were variously used as outer container in the present work. Fig. 30 shows the first cell design used; it is similar to that described by Hollingshead and Braunwarth (19). Airburn of the cathode crucible was minimised by circular, segmented, sintered alumina bricks, with a 3in diameter central opening to allow insertion and removal of anode samples. Above the alumina brickwork rested a similar set of porous silica bricks, with the whole refractory assembly contributing to the minimizing of heat losses from the cell contents. Dimensionally, each cathode was 8in high with an internal diameter of 6in, and a base thickness of 1in; the refractory bricks were each 1in thick.

The 2in diameter anodes were threaded directly to 3/8in diameter copper rods. These rods were notched

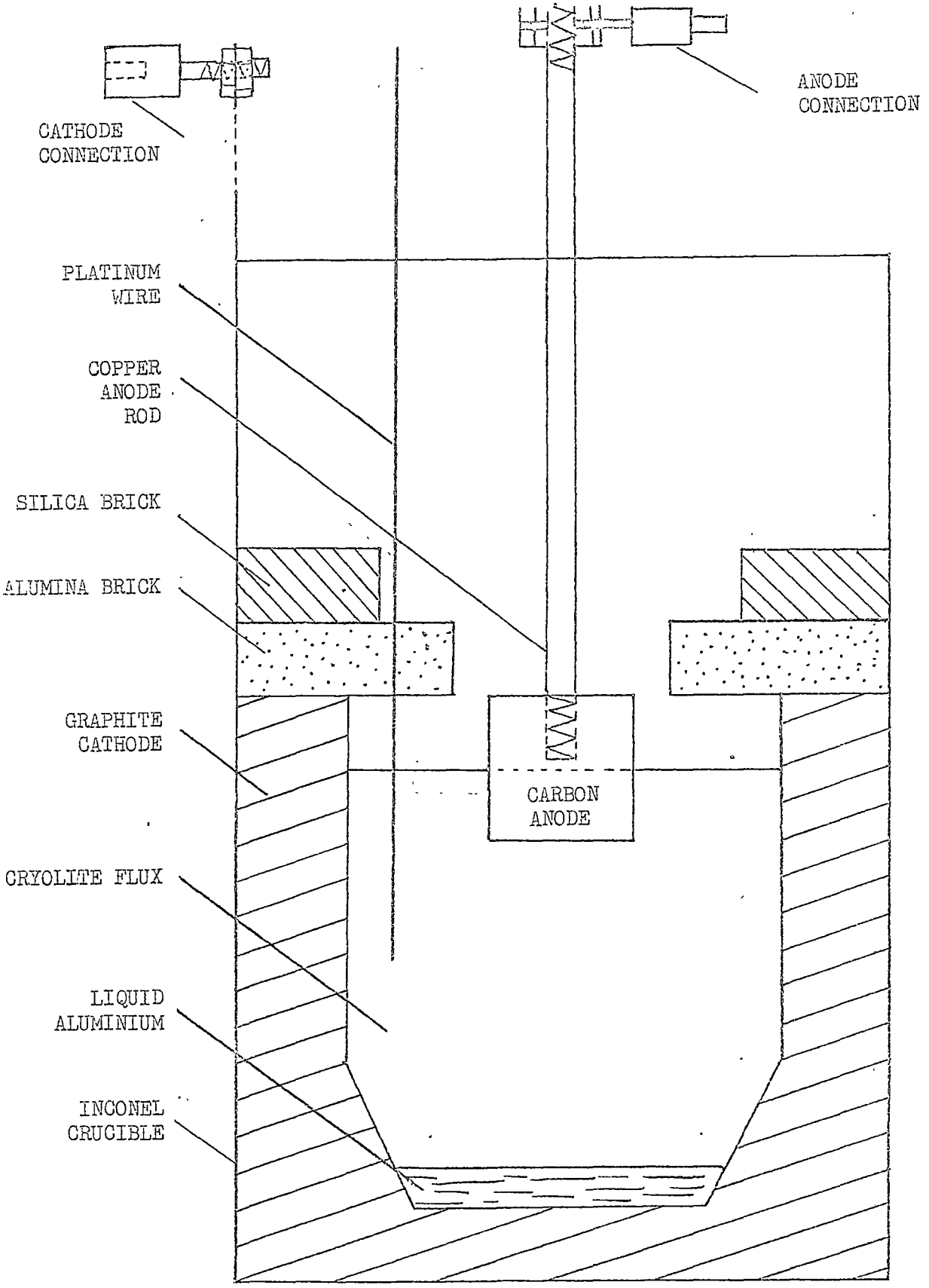

FIGURE 30

EXPERIMENTAL ELECTROLYTIC CELL
CONSTRUCTIONAL DETAILS
(HALF SCALE)

every ¼in along their entire length to assist in determining the extent of immersion of the anode in the molten electrolyte.

Electrical connections were made to the cell through snap-on heavy duty connectors designed to take direct currents of up to 100A. Similar connectors were used on the upper ends of the anode rods.

Provision was also made for measuring the voltage drop between the anode rod and the electrolyte by inserting a 26 gauge platinum wire below the melt surface, halfway between anode and cathode. The purpose of this was to measure the effect of anode additives on this component of the overall cell voltage.

The whole assembly was contained in a 7.5KVA resistance-heated furnace; cell and furnace were maintained under an argon atmosphere to prevent oxidation, and covered by a "Miscolite" cover to reduce heat losses. Temperature control was achieved by a variable autotransformer, and a "Pyrotenax" chromel-alumel thermocouple placed between the cell and the furnace element, operating a Cambridge temperature indicator-controller of the on-off variety.

A second type of reduction cell which was used in the later stages of this work is shown in Fig. 30a. The major points of alteration are a reduction in

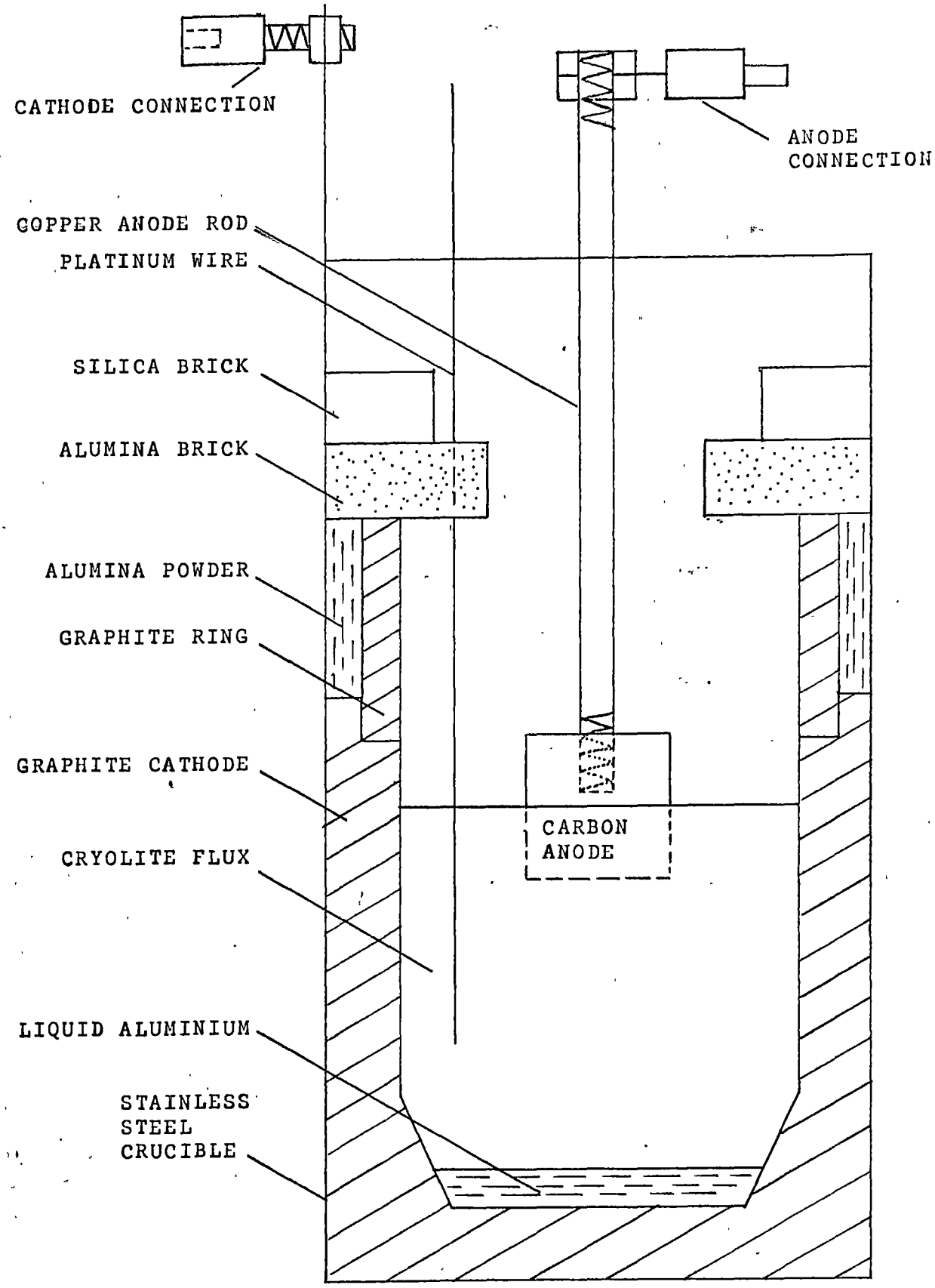

Figure 30a (Half scale)

EXPERIMENTAL ELECTROLYTIC CELL - CONSTRUCTION DETAILS

diameter from 9in to 7.5in, and the provision of a graphite ring above the crucible. The size reduction was in the interests of general ease of handling and the accommodation within the 11½in (maximum diameter) hexagonal heating furnace, and the graphite ring was to contain a layer of alumina which was intended to prevent airburn of the crucible rim. No other detailed changes other than dimensions, were altered in this smaller cell.

The direct-current supply for electrolysis was provided by a full wave germanium rectifier unit, designed to provide a maximum of 350 amperes at 12 volts. This rectifier was operated through a heavy duty oil-filled transformer (minimum setting 22V) and a 2.5 KVA variable autotransformer. Electrolysis current was measured by a 0 - 100A ammeter (graduated in 2A divisions), while overall cell voltage was measured on 0 - 10V meters (graduated in 0.4V divisions) and the anode-to-flux voltage component was determined on 0 - 2V meters (0.1V divisions). These meters were all of the conventional five inch square type.

(ii) Raw Materials for Cell.

The materials used in the electrolyte were normal industrial-grade materials, and were sieved through a 48 mesh Tyler sieve prior to use to remove coarse particles of impurities. Following this treatment, each component of the electrolyte was analysed for

iron and silicon, contaminants considered detrimental in practice. (See Appendix "A" for all analytical details).

The analytical results obtained are listed hereunder:

Cryolite	Fe	0.01%	
	Si	0.11%	
	Na	33.6%	(calc. 32.9 for Na_3AlF_6)
	NaF/AlF_3 - ratio	1.44%	
	Free Al_2O_3	0.87%	(after ignition at 900°C)
Aluminium Fluoride	Fe	0.01%	
	Si	0.17%	
	Al	29.7%	(calc. 32.1 for AlF_3)
Calcium Fluoride	Fe	0.05%	
	Si	0.11%	
	CaF_2	97.5%	
Alumina	Fe_2O_3	0.015%	
	SiO_2	0.016%	
	Na_2O	0.60%	

From these raw materials, a bath of the following nominal composition was prepared:

CaF_2	8.0%
Free Al_2O_3	4.0%
NaF/AlF_3 ratio	1.40% (by weight)

This composition is within the normal operating range for cryolitic electrolyte for aluminium reduction furnaces. Such a mixture has the following properties (21):

Freezing Point	958°C
Density	2.145 gm/cm^3 at 975°C
Specific Conductivity	2.31 ohm^{-1} cm^{-1} at 975°C.

10Kg quantities were prepared at a time, using the same mixer which was used to prepare the carbon anode mixtures.

(iii) Cell Operation

For the various phases of work using the laboratory cell, the preparation of the apparatus was similar. 3,500g of prepared flux was placed on top of 300g of aluminium, and the refractory brickwork placed on the crucible rim. The platinum wire used for anode-flux voltage drop measurements was inserted into the powdered flux halfway between anode and cathode, so that approximately 2in of the wire was beneath the surface when the bath was molten.

After fitting the assembled cell into the heating furnace, and placement of the controlling thermocouple, a small hollow "Fibrefrax" Al_2O_3 - SiO_2 refractory cone was placed base down on the alumina brickwork, and the protective argon atmosphere introduced through a stainless steel tube through the ½in hole at the apex of the cone.

When the cell contents, during warm-up, had attained 500°C, the argon atmosphere was admitted at a constant flow-rate of 100 S.T.P. ml/min.

Normally the apparatus was brought to its operating temperature (approximately 980°C) overnight, as the time taken for the entire sit-up to reach this temperature, at the maximum heating rate, was four to five hours in the case of the smaller cell. This does not include the time to melt the flux after reaching operating temperature. When the flux was completely molten, the appropriate anode assembly was introduced, the electrolysis circuit completed and readings commenced.

Three main types of measurement were made in this section of the investigation. These were:-

Current-voltage measurements

For anodes of a variety of compositions, measurements were made of corresponding values of cell current and overall cell voltage. In practice, the selected anode was screwed to the copper rod, and fastened into its supporting clamp. Before immersion of the anode in the electrolyte, the rectifier set was switched on, and adjusted to a d.c. output of an arbitrary 3.3V (open circuit).

The contact point of the anode and flux was determined by observing the point at which the electrolytic circuit was completed, as detected on the meter panel, and then measuring further immersion by the notches of the anode rod. (Normally, immersion of 1in was sought; this could be checked by measurement of the thin line of frozen

crust on the anode at this level after removal from the bath at the end of the run.)

After immersion at the desired depth, a stabilizing period of ten to fifteen minutes was allowed to permit the newly-frozen flux on the anode to remelt. The end of this period was determined from the constancy of the decreasing cell voltage and the increasing current. From this point on, the electrolysis voltage was manually increased using the variable transformer, up to the point where a current of 90 - 100A was flowing. To test the reproducibility of results, the voltage was then lowered gradually, to the minimum obtainable, and finally increased to its original value.

From the results obtained from this procedure, comparisons between anode materials could be made.

Critical current density measurements.

In this work, anodes of less than 1in diameter were prepared by machining larger electrodes (for actual dimensions see Results section) to achieve anode current densities considerably higher than in the current-voltage runs. The procedures of the previous section were followed, and current-voltage readings taken at regular intervals. At a certain anode current density, results similar to those of Welch and Snow (22) were expected, wherin a sudden large drop in current occurs along with an increase in voltage. These conditions

indicate the onset of "anode effect", and a comparison of the conditions under which it is initiated can be considered as a measure of the efficiency of the various additives in promoting adhesion between electrolyte and anode.

Current efficiency and carbon consumption.

Extended electrolyses were performed, representing the passage of up to 15 Faradays at a nominal current density of 1 A/sq cm.

The weights of the anode before and after electrolysis were obtained, and by correction for the ash content of the anode, total carbon consumption was calculated.

The determination of the quantity of electricity was made by two methods. The first of these used the area under the graph of current against time; the second involved averaging the current in selected time intervals, and thus calculating the total Faradic flow. A comparison of these two methods showed them to agree within an average of 1.2%.

(d) Results.

(i) Operation of Reduction Cell.

During the course of this study, it was confirmed that certain difficulties occur in the operation of externally heated aluminium reduction cells. These arise mainly through the combination of high temperature and corrosive electrolyte, causing short service life of cell components due to corrosion and oxidation. In addition, the "freeze-and-thaw" mode of operation causes a gradual deterioration of the cathode crucible.

Initial work with the cell made use of a cathode crucible machined from a crystalline carbon block originally supplied for building industrial aluminium furnaces. An attempt was made to "condition" this material by immersion in molten cryolite for 48 hours, in order that preferential absorption of sodium compounds would take place. However, this type of carbon proved to be unsuitable in service, either with or without conditioning, as its macrocrystalline structure allowed flux seepage, and the subsequent melting and solidification cycle of operation caused penetration of the flux to the outer metal container, resulting in corrosion and service failure. (Fig. 31)

Following the above experience, a graphite cathode was employed. The main advantage of this material lay in its higher purity and dense structure, with greatly

reduced penetration by the electrolyte.

Although a steady stream of argon was maintained in the cell during operation, oxidation of the cathode above the flux line slowly occurred, resulting in the need for its eventual replacement. Where the cathode could be removed in one piece, it was later split in halves to examine the extent of flux penetration. This is shown in Fig. 32.

In practice, replacement of the cathode was as a result of airburn, rather than flux penetration, causing only slight corrosion of the metal container.

The tendency of cryolitic melts to fume is a cause of operating difficulties and corrosion in this type of apparatus, in that corrosion of the metal container between the cathode and the alumina brickwork occurs. This trouble could be corrected by inserting a stainless steel sleeve, 0.019in thick and 3in high, between the brickwork and the outer crucible. This sleeve was replaced after each run and its use prevented corrosion of the container in this region.

Throughout the work, a gradual corrosion of the sintered alumina bricks in the cell took place, caused by fuming of the electrolyte. Although this was undesirable, no real difficulties were encountered, and other available materials were considered to be less suitable. No problems were encountered with the upper layer of

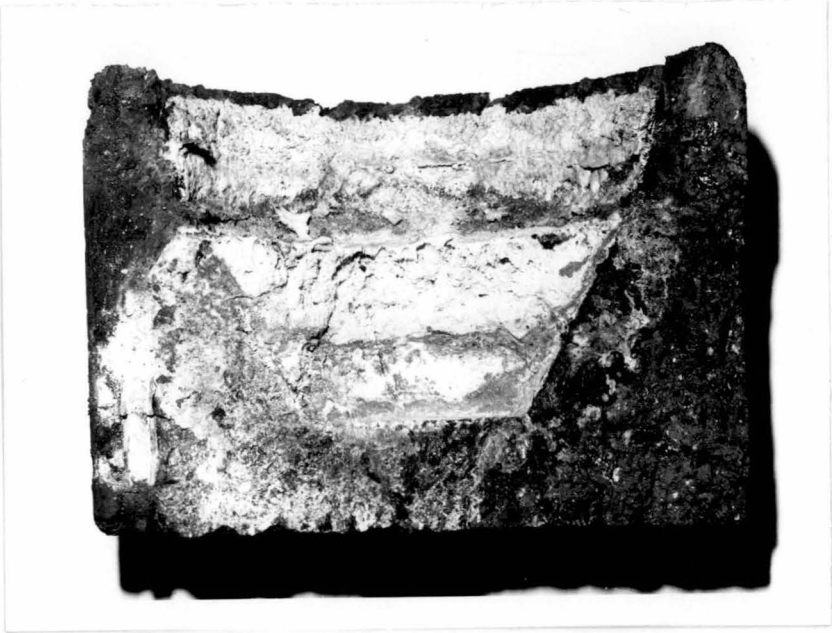

Figure 31: Penetration of flux to outer surface of crystalline carbon cathode.

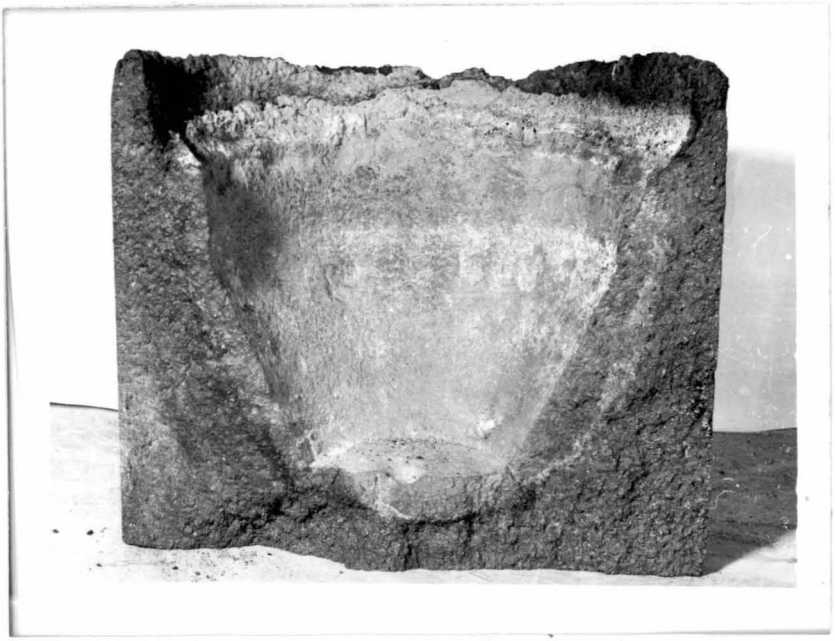

Figure 32: Penetration of flux into graphite cathode after prolonged use in experimental cell.

brickwork in the cell. The silica segments were coated with refractory wash, which prolonged their useful life.

In the early stages of cell operation, the outer metal containers were of Inconel alloy. Later these were replaced by stainless steel containers which were equally satisfactory.

(ii) Current-Voltage Measurements.

In evaluating the efficiency of additives to the anode mixture from the nature of the current-voltage graphs, a number of factors must be considered. These include:-

(1) The decomposition voltage, V_o, i.e., the value of the overall cell voltage when extrapolated to zero current flow.

(2) The slope of the linear portion of the graph above V_o.

(3) The anode-flux voltage drop. This has been referred to as the "overvoltage", and although the measurements made in this work are not those of a true overvoltage but rather of an empirical operating variable, the anode-flux interfacial conditions nevertheless make a significant contribution to the overall cell voltage in practice.

(4) Cell voltage at a specific anode current density. Normal furnace operation is at an anode current density

of the order of 1 A/sq cm, and this figure can be used as a basis for comparative evaluation in this work.

To determine the values of the above variables, notably (1), (2), and (4), a least squares method was employed over the linear portion of the current-voltage graphs.

The following tables of results, with their appended comments, refer to typical results of current-voltage runs and anode-flux voltage drops, using both plain and modified anodes.

Table 1: Effect of additives on overall cell voltage.

Additive in anode	V_o (volts)	Slope (amps/volt)	Cell voltage at 1A/sq in (current = 66A)
Nil	1.26	28.3	3.59
5% Al_2O_3	1.37	33.5	3.34
10% Al_2O_3	1.39	27.6	3.74
25% Al_2O_3	1.40	27.1	3.83
2% $CaCO_3$	1.32	28.8	3.61
1% CaF_2	1.42	31.6	3.51
2% Cryolite	1.42	32.8	3.43
2% LiF	1.23	31.9	3.30
2% Li_2CO_3	1.33	30.5	3.50

Comments:

Anode immersion 1⅛in

Flux temperature 980 ±5°C

Flux composition CaF_2 = 6.3%
Free Al_2O_3 = 4.3%
NaF/AlF_3 ratio = 1.39

Al_2O_3 at 10% and 25% levels added as kiln dust, approx. 85% -325 mesh (Tyler).

Table 2: Effect of additives on overall cell voltage.

Additive in anode	V_o (volts)	Slope (amps/volt)	Cell voltage at 1A/sq in (current - 66A)
Nil	1.54	25.50	4.13
2% Al_2O_3	1.44	26.28	3.85
2% Li_2CO_3	1.59	36.90	3.62
Nil	1.43	25.23	4.56
2% Al_2O_3	1.63	34.75	3.79
2% Li_2CO_3	1.56	28.22	3.90

Comments:

Anode immersion $1\frac{1}{8}$in approx.

Flux temperature 980 $\pm 5^{\circ}$C

Flux composition CaF_2 = 6.1%
Free Al_2O_3 = 5.7%
NaF/AlF_3 ratio = 1.46

Table 3: Effect of additives on anode-flux voltage.

Additive in anode	Anode-flux voltage at 1A/sq cm (current=66A.)	Anode-flux voltage at 1A/sq cm (current=22A.)
Nil	1.27	1.18
5% Al_2O_3	1.19	0.96
10% Al_2O_3	1.39	0.90
25% Al_2O_3	1.41	1.13
2% $CaCO_3$	1.20	1.12
1% CaF_2	1.07	0.95
2% Cryolite	0.97	0.80
2% LiF	1.24	0.98
2% Li_2CO_3	1.36	1.02

Comments:

Anode immersion: at 66A, immersion = 1⅛in

at 22A, immersion = zero
i.e., only face of anode in contact with electrolyte.

Other details as for Table 1.

Table 4a: Anode Flux Voltages prior to current-voltage runs.

Additive in anode	Anode-Flux Voltage	Total Voltage	Current (amps)
Nil	1.05	2.5	21
5% Al_2O_3	0.95-1.0	2.6	22
10% Al_2O_3	0.95	2.6	23
25% Al_2O_3	1.0	2.7	18
2% $CaCO_3$	0.85	2.65	18
1% CaF_2	0.85	2.6	19
2% Cryolite	0.82	2.6	24
2% LiF	1.01	2.55	24
2% Li_2CO_3	0.98	2.45	22

Comments:

Anode immersion: Interfacial contact only.

Other details as for Tables 1 and 2.

The readings refer to stable values obtained, for constant rectifier settings, after the flux at the anode face had remelted. This required approximately 10 minutes after immersion of the anode in the melt.

Table 4b: Anode-Flux Voltages prior to current-voltage runs.

Additive in anode	Anode-Flux Voltage	Total Voltage	Current (amps)
Nil	0.80	2.5	29
Nil	0.78	2.5	27
10% Al_2O_3	0.79	2.5	29
25% Al_2O_3	0.92	2.5	28
25% Al_2O_3	0.95	2.7	24
2% LiF	0.76	2.4	33
Nil	0.82	3.1	29.5
1% Al_2O_3	0.68	2.8	41
5% Al_2O_3	0.70	2.8	40
2% Li_2CO_3	0.68	2.8	33.4

Comments:

Anode immersion ½in

Flux temperature 980 ±5°C

Flux composition CaF_2 = 4.2%
Free Al_2O_3 = 5.8%
NaF/AlF_3 ratio = 1.47

Of the above ten readings, the first six were measured in one series of runs, the next four in a second series. The readings were taken after the interfacial flux had melted (as in Table 4a).

Table 4c: Anode-Flux Voltages prior to current-voltage runs.

Additive in anode	Anode-Flux Voltage	Total Voltage	Current (amps)
Nil	1.31	2.35	26
1% Al_2O_3	0.59	2.35	24
2% Al_2O_3	0.48	2.35	25
5% Al_2O_3	0.45	2.35	24
10% Al_2O_3	0.56	2.20	23
25% Al_2O_3	0.79	2.45	20
50% Al_2O_3	0.78	2.40	25
1% CaF_2	0.55	2.40	26

Comments:

Anode immersion 1in

Flux temperature 980 ±5°C

Flux composition CaF_2 = 7.0%
Free Al_2O_3 = 11.9%
NaF/AlF_3 ratio = 1.47

The readings in this table were taken consecutively on the same day, and the composition of the flux remained sensibly constant during the series, with the change in alumina concentration being less than 1% absolute.

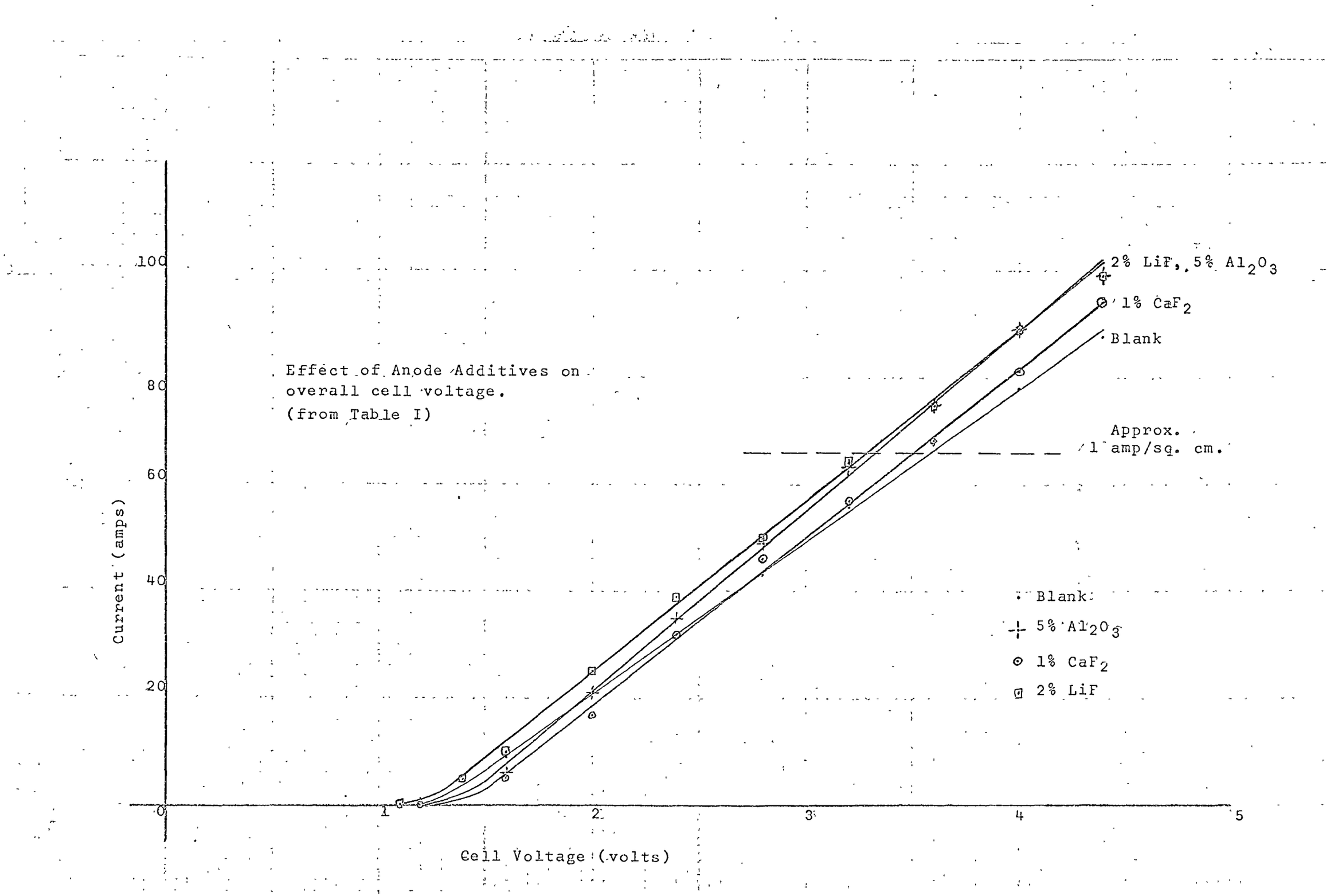
Effect of Anode Additives on overall cell voltage.
(from Table I)
Current (amps)
Cell Voltage (volts)
0
20
40
60
80
100
1
2
3
4
5
2% LiF, 5% Al_2O_3
1% CaF_2
Blank
Approx. 1 amp/sq. cm.
Blank
5% Al_2O_3
1% CaF_2
2% LiF

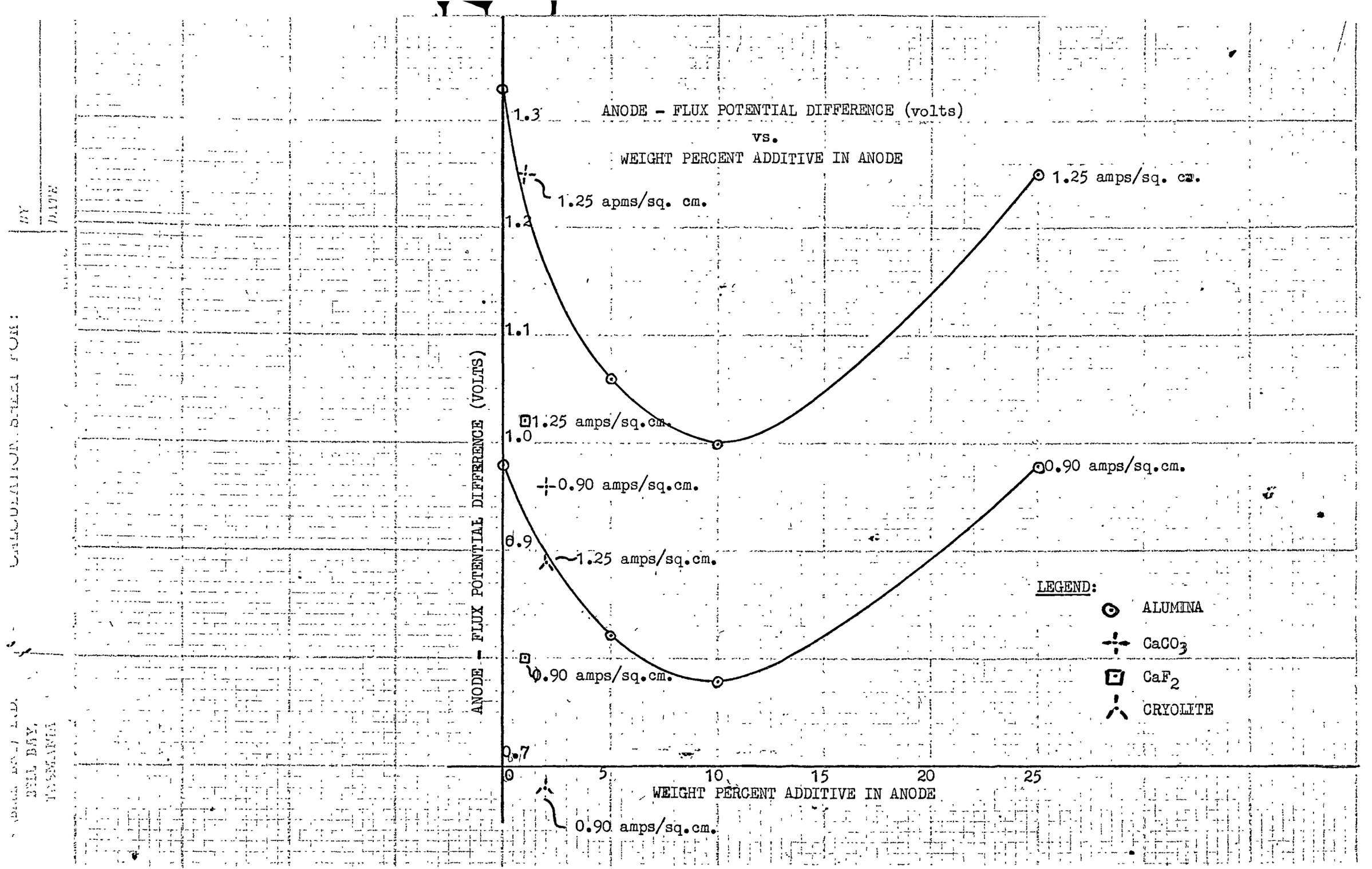
ANODE - FLUX POTENTIAL DIFFERENCE (volts)
vs.
WEIGHT PERCENT ADDITIVE IN ANODE
1.25 apms/sq. cm.
1.25 amps/sq. cm.
1.25 amps/sq.cm.
0.90 amps/sq.cm.
0.90 amps/sq.cm.
1.25 amps/sq.cm.
0.90 amps/sq.cm.
0.90 amps/sq.cm.
LEGEND:
ALUMINA
$CaCO_3$
CaF_2
CRYOLITE
ANODE - FLUX POTENTIAL DIFFERENCE (VOLTS)
1.3
1.2
1.1
1.0
0.9
0.7
0
5
10
15
20
25
WEIGHT PERCENT ADDITIVE IN ANODE

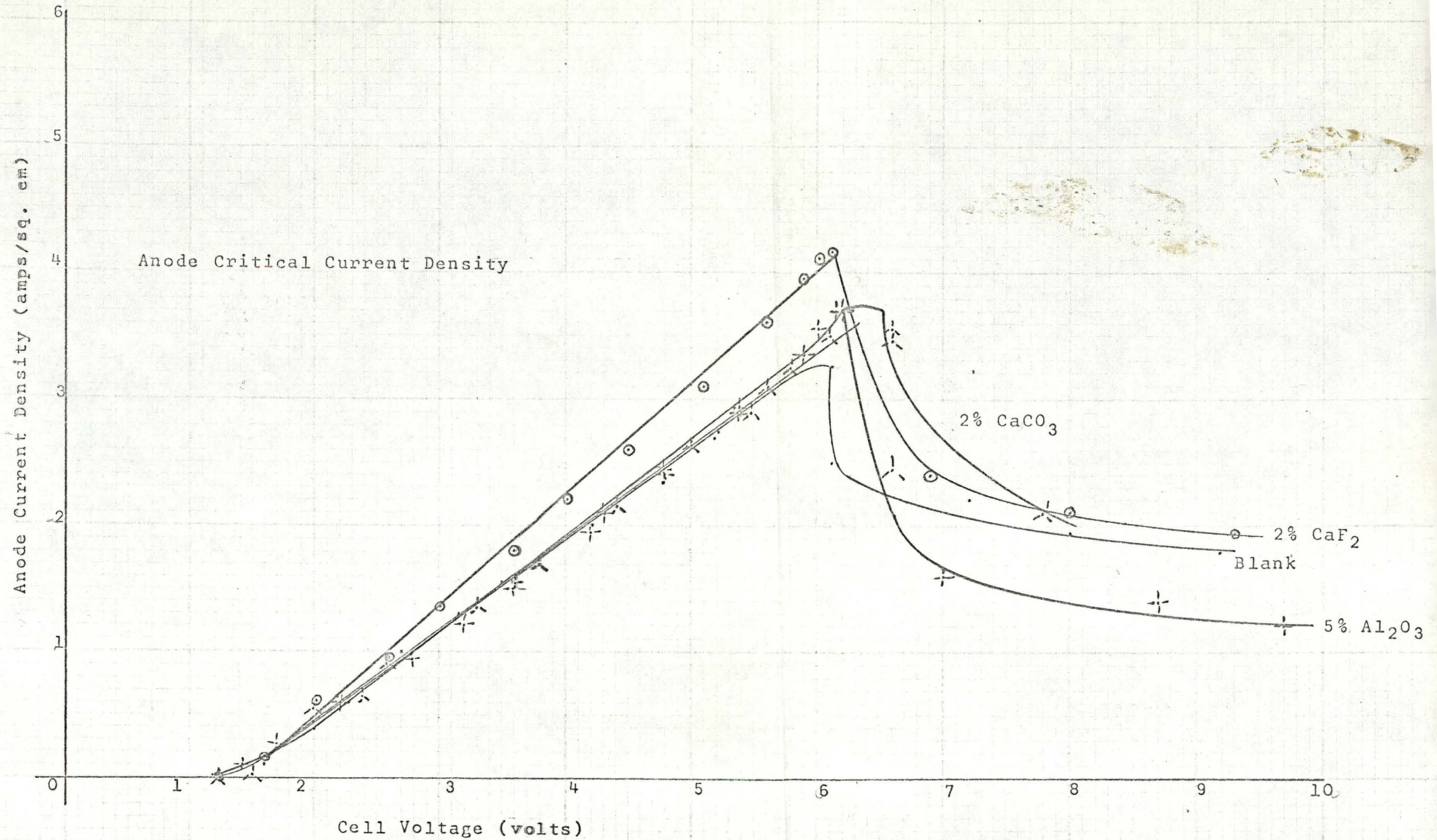
Anode Critical Current Density
Anode Current Density (amps/sq. cm)
Cell Voltage (volts)
0
1
2
3
4
5
6
7
8
9
10
2% $CaCO_3$
2% CaF_2
Blank
5% Al_2O_3

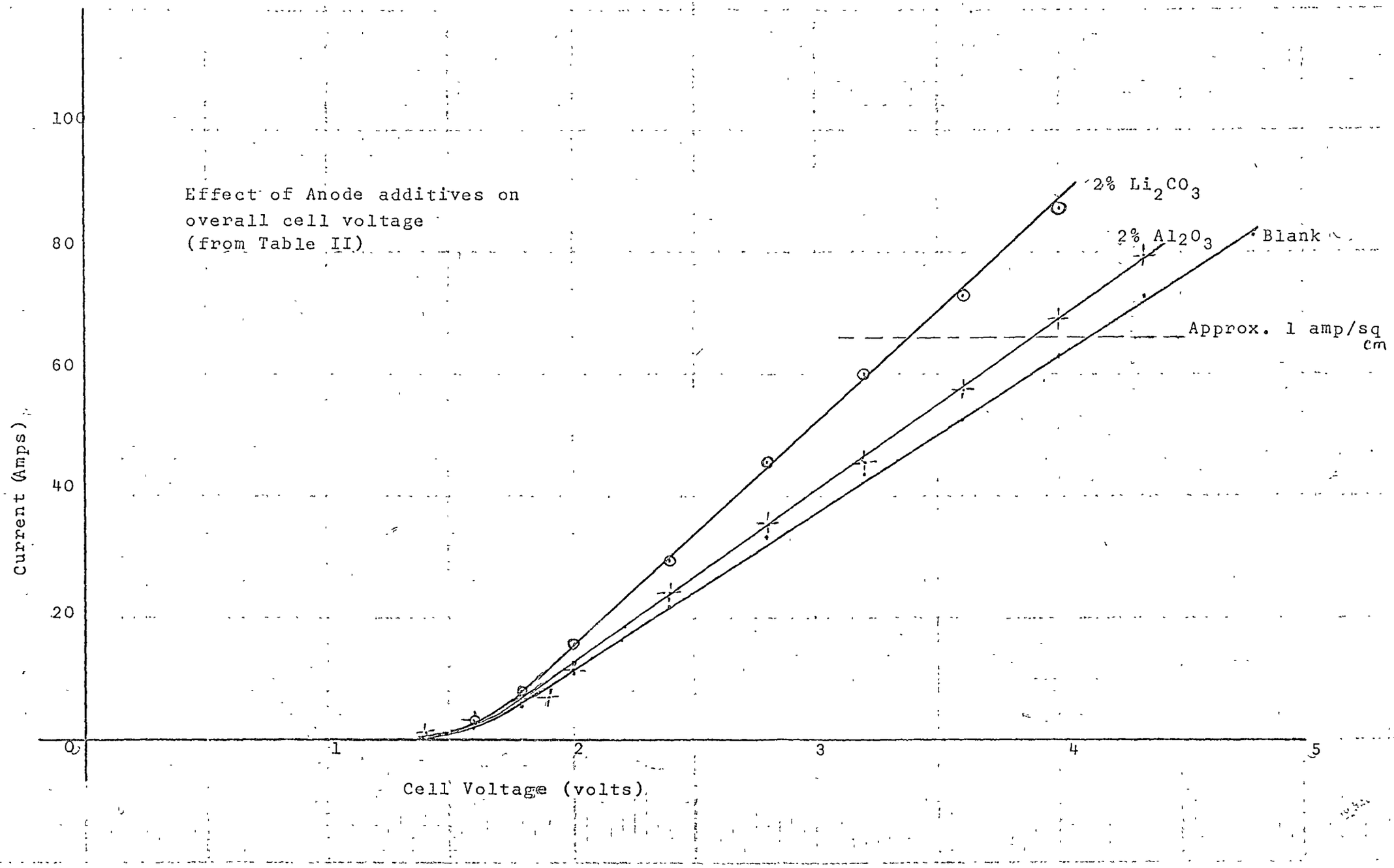
Effect of Anode additives on
overall cell voltage
(from Table II)
2% Li_2CO_3
2% Al_2O_3
Blank
Approx. 1 amp/sq cm
Current (Amps)
Cell Voltage (volts)
0
20
40
60
80
100
1
2
3
4
5

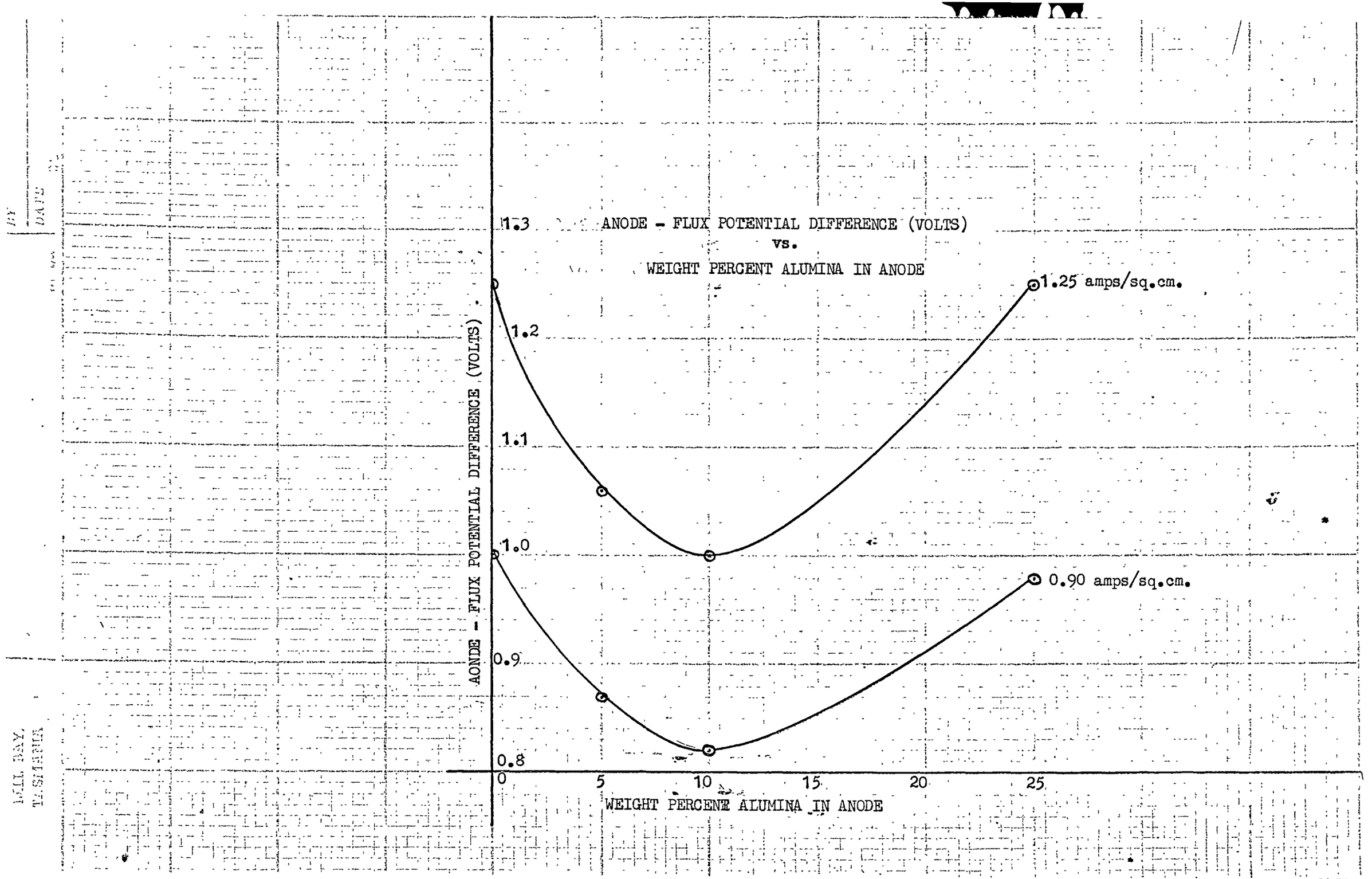
ANODE - FLUX POTENTIAL DIFFERENCE (VOLTS)
vs.
WEIGHT PERCENT ALUMINA IN ANODE
1.25 amps/sq.cm.
0.90 amps/sq.cm.
AONDE - FLUX POTENTIAL DIFFERENCE (VOLTS)
1.3
1.2
1.1
1.0
0.9
0.8
0
5
10
15
20
25
WEIGHT PERCENT ALUMINA IN ANODE

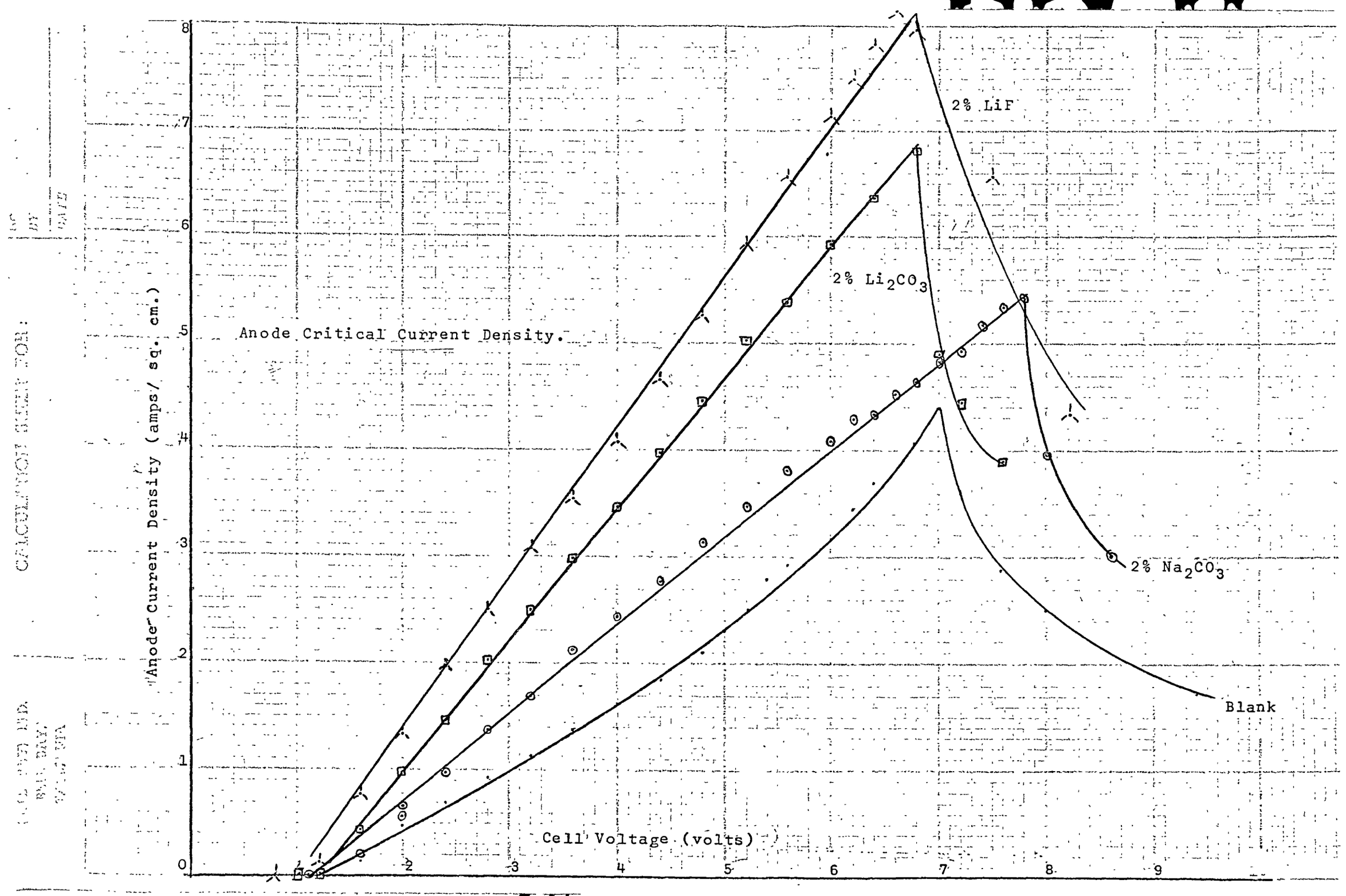
Anode Critical Current Density.
Anode Current Density (amps/ sq. cm.)
Cell Voltage (volts)
2% LiF
2% Li_2CO_3
2% Na_2CO_3
Blank
0
1
2
3
4
5
6
7
8
9

(iii) Critical Current Density Measurements.

In making these measurements, it was found that, as the anode effect conditions were approached by increasing the current and voltage, the readings became rather unstable. When the anode effect did occur, it took the form of a rapid drop in current and a corresponding increase in cell voltage. The maximum current density and voltage observed under conditions of smooth conduction in the various instances are listed in the following table.

Table 5: Critical Current Density Conditions

Additive in anode	Anode Diameter	Anode effect conditions	
		Maximum voltage	Anode current Density (A/sq cm)
Nil	19mm	5.6	3.15
2% Al_2O_3	"	6.0	3.1
5% Al_2O_3	"	6.2	3.7
2% Li_2CO_3	"	5.6	3.6
2% $CaCO_3$	"	6.6	3.55
2% CaF_2	"	6.1	4.15

Table 5 continued.

Additive in anode	Anode Diameter	Anode effect conditions	
		Maximum voltage	Anode current Density (A/sq cm)
Nil	26mm	6.6	3.9
2% Na_2CO_3	"	7.8	5.4
2% $CaCO_3$	"	7.0	6.9
2% Li_2CO_3	"	6.8	6.8
2% LiF	"	7.2	8.4
2% CaF_2	"	8.3	6.3
2% AlF_3	"	6.6	4.3
1% Al_2O_3	"	6.7	3.9
5% Al_2O_3	"	6.4	4.2

(iv) Current Efficiency and Carbon Consumption.

In long term operation, of periods up to eight hours, no major problems were encountered in reduction cell operation. In such operations as were needed to provide data on the relationship of current efficiency to block composition, for other constant cell conditions, a number of features were noted in each run. These were:-

1) A progressive diminution of immersed anode surface area as electrolysis proceeded. This took the form

of a reduction in the area of the immersed anode face and a reduction in the depth of immersion of the anode in the electrolyte. Consequently an increase in the anode to cathode distance resulted. Generally, the tendency was for the originally cylindrical anode to approach a hemispherical shape as the run extended. Typically, the reduction in immersed surface area of the anode was from 60 sq cm to about 40 sq cm for the passage of approximately 15 Faradays through the system. At the same time, the depth of anode immersion in the melt was reduced by about $\frac{1}{4}$in.

2) A gradual decrease in current and a corresponding increase in cell voltage for constant apparatus settings. This was more noticeable during the latter stages of a given electrolytic run, and was ascribed to the increase in anode-cathode distance in the melt.

3) The long term instability of the anode-to-flux voltage drop. In the majority of cases this measurement showed an irregular rise and fall pattern. Because of this, the anode-flux voltage drop could not be used as a continuous operating parameter for the basis of comparisons between anodes. Only in the short term runs could these values be used to compare different anodes, as in Section (ii). An explanation

advanced for such a behaviour is that the short range effects of changes in alumina concentration in the electrolyte in relation to the overall dimensions of the cell have caused composition gradients, resulting in varying voltage components in the anode-flux region. This suggestion is supported by the fact that agitation of the electrolyte by vertical movement of the anode assembly caused variation in the anode-flux voltage drop, as did a rotation or oscillation of the anode.

4) The behaviour of the cell when operated until occurrence of "anode effect". This phenomenon is a function of alumina concentration and anode current density, and in long-term cell operation was obtained as a sudden drop in current from approximately 50A to 15A, and corresponding voltage increases of from 3.6 - 3.7V to 4.6 - 4.8V. No modification of cell operation or stirring of electrolyte would cure this condition. Adding alumina was not attempted at these times, but additional evidence for the anode effect was found in the smooth appearance of the anode surface, with no adhering flux on removal from the melt.

5) The variation in cell current obtainable by anode movement. In the observed instances of slowly

decreasing cell current, a sideways movement of the anode caused a temporary rise in current of 2 - 3A. This is probably due to the release of small gas bubbles from below the anode.

The following tables show how anode composition is related to current efficiency and carbon consumption in extended experiments:-

Table 6: Effect of Anode Composition on Current Efficiency.

Additive in anode	Current Efficiency %
Nil	88.4
1% Al_2O_3	95.2
2% Al_2O_3	92.0
5% Al_2O_3	92.0
10% Al_2O_3	102.7
25% Al_2O_3	77.7
1% CaF_2	99.7
2% CaF_2	90.6
2% $CaCO_3$	94.5
2% Na_2CO_3	95.6
2% LiF	96.7
2% AlF_3	85.2
2% Li_2CO_3	94.3

Table 7: Carbon Consumption in relation to Anode Composition.

Additive in anode	% of Theoretical Carbon Consumption	Carbon Ratio *
Nil	113.1	0.377
1% Al_2O_3	105.1	0.350
2% Al_2O_3	108.7	0.362
5% Al_2O_3	108.7	0.362
10% Al_2O_3	97.4	0.325
25% Al_2O_3	128.7	0.429
1% CaF_2	100.3	0.334
2% CaF_2	110.4	0.368
2% $CaCO_3$	105.8	0.353
2% Na_2CO_3	104.6	0.349
2% LiF	103.4	0.345
2% AlF_3	117.4	0.391
2% Li_2CO_3	106.0	0.353

* Theoretical carbon ratio = 0.333 at 100% current efficiency, corresponding to the reaction:

$$2Al_2O_3 + 3C = 4Al + 3CO_2$$

(e) Discussion

The results obtained in working with laboratory reduction cells indicate that in many cases the addition of inorganic additives to carbon anodes has brought improved performance under electrolytic conditions. The effect of such additives at practical current densities of approximately 1A/sq cm is shown in the accompanying graphs and it is apparent that a lowering of more than 0.5V can be realised under laboratory conditions when 2% Lithium Carbonate is included in the anode.

Tables 1 and 3 show that when larger amounts of additives such as 10% and 25% of alumina are used in the anodes, an increase in both total cell voltage and anode-rod-flux voltage is observed. This is attributed to the higher specific resistance of such anodes, a feature detrimental in practice in spite of good physical adhesion of electrolyte. Measurements of carbon consumption relative to the total amount of electricity passed through the cell for determination of current efficiency show that for many modified anodes, the effect of the additive has been to reduce the anode consumption per Faraday. Although no uniform trend is indicated, the experimental evidence suggests that improved interfacial adhesion has been beneficial in cell operation.

In the case of 25% alumina anodes, an increase in carbon consumption has occurred. It is considered that such a high amount of additive has caused discontinuities in the carbon anode, and the resulting increased internal carbon surface has promoted formation of carbon monoxide in the anode gases. This follows from the assumption that good interfacial contact assists penetration of the carbon by the electrolyte, and consequently electrolysis proceeds within the anode as well as at the surface. Carbon dioxide released within the hot anode could then form some carbon monoxide prior to release from the cell.

The distribution of inorganic additives throughout an amorphous carbon matrix can be broadly likened to a mixture of spherical particles of two differing materials. When uniform spheres are close-packed, a void space results comprising 25.9% of the total volume. This void space can contain a similar amount of a second material without disturbing the continuity of the host lattice. Higher amounts will cause discontinuities, until a "reversal" will occur when the intruding phase becomes continuous.

In the present case, we are dealing with a matrix of non-uniform aspherical carbon grains, and in practice the void space in the electrodes is approximately 10-15%. Thus, additive materials used, which are generally -100 mesh particles, can be included in the electrodes

in similar quantities (10 - 15%) without breaking up the carbon matrix. This particular feature is considered further in Appendix "B", in examining the electrical properties of the anode materials.

Using aluminium fluoride as an additive at the 2% level, the result is of the same order as a plain anode. This compound differs from the other additives in that, rather than containing discrete ions in its structure, it consists of an extended three-dimensional network of $[AlF_6]$ octahedra joined at their apices (23). Each fluoride ion is then shared by two octahedra, and the overall structure is of 6 : 2 co-ordination, with each aluminium ion surrounded by six fluoride ions (Fig. 33).

This contrasts with the fluorite structure, the unit cell of which contains individual ions (Fig. 34). Similar considerations apply to the other anode additives used, in that they have unit cells consisting of discrete cations and anions. The graphite structure (Fig. 35), by comparison, contains the well-known hexagonal arrangement of carbon atoms joined by covalent bonding.

Because of the general structural difference between aluminium fluoride and the electrolyte the adhesion between a cryolite flux and an anode containing aluminium fluoride additive is similar to that occurring with an unmodified anode. The contact angle measurements and

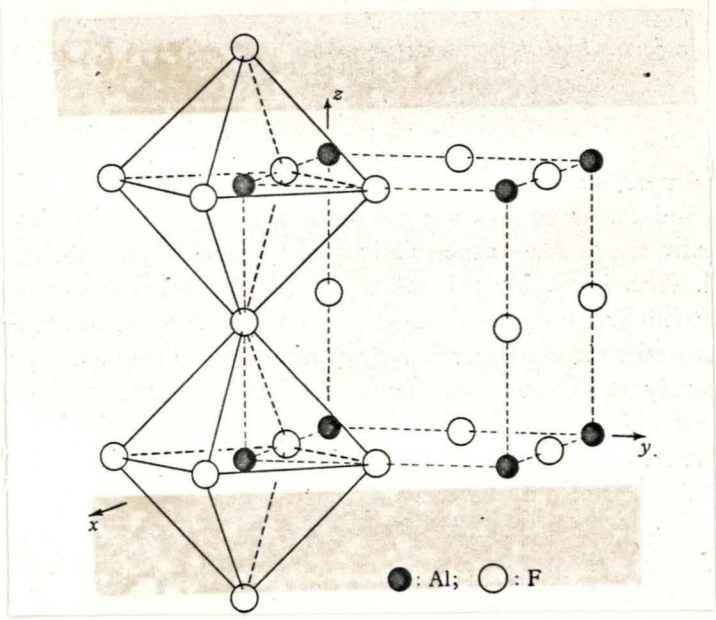

Figure 33: Unit cell of the cubic AlF_3 structure, showing linkage of $[AlF_6]$ octahedra at their corners.

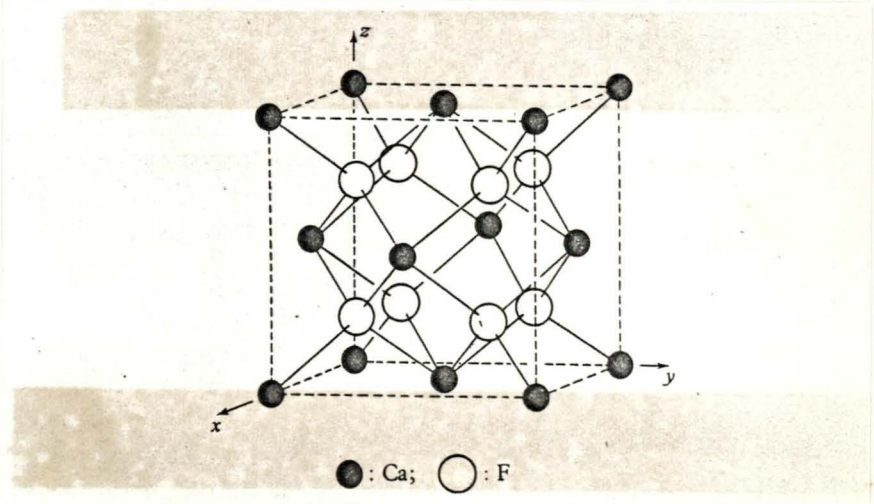

Figure 34: Unit cell of the cubic fluorite structure, CaF_2.

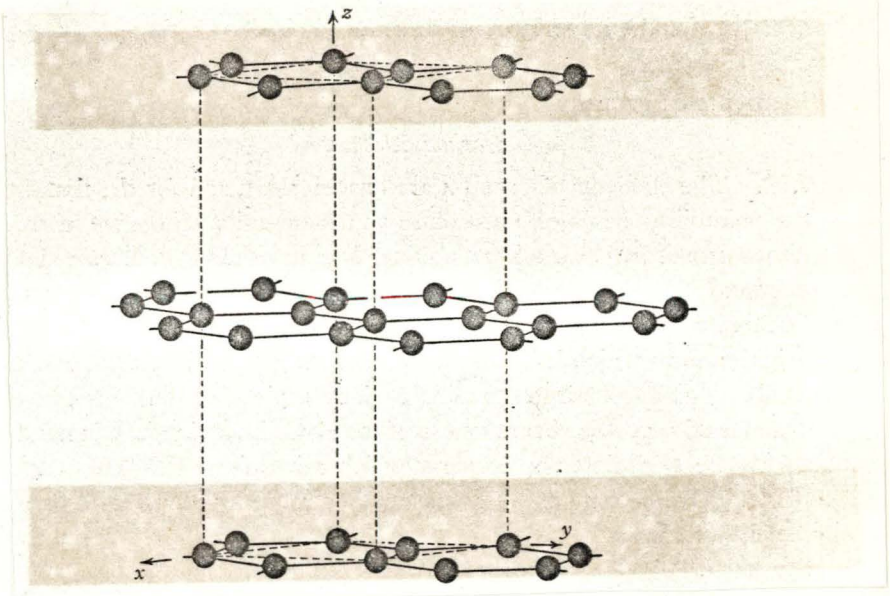

Figure 35: Unit cell of the hexagonal structure of graphite.

observations also support this hypothesis, in spite of the fact that the actual Al - F bond is approximately 62% ionic (23).

The critical current density results provide additional evidence that improved interfacial contact results from modification of the anode composition.

After an anode effect had been induced, reproducible current-voltage results could not be obtained immediately. The reasons are probably two-fold. It is known (24) that one of the features of the anode effect is the presence of an insulating layer of material, sometimes designated as $(CF)_n$, covering the immersed anode surface. Until this insulation is removed and the original anode-flux contact established, reproducible results cannot be expected. Also, the presence of an anode effect can cause a local heating of several hundred degrees Centigrade (6), and the presence of thermal gradients within the cell will alter the corresponding current and voltage values until equilibrium is again established.

During the anode effect, small arcs could be observed between the anode and the electrolyte, a characteristic of cell operation under these conditions.

In practice, anode current densities of the magnitude listed in the results are not achieved. However, the conditions required to interupt smooth conduction are an indication of the mutual affinity of the two phases.

PART III : CONCLUSION

(a) Preliminary Plant Measurements.

In predicting the potential value of the foregoing work on an industrial basis, measurements have been made of certain voltage components of operating aluminium reduction furnaces. For the 48,000A cells of Comalco's Bell Bay smelter, the design permits measurements of interfacial voltage drops between the carbon anode and the cryolite flux to be made readily. The results of such measurements can serve as an indication of scope for improvements in cell operation as a result of improved wettability of anodes which have been modified by the additives mentioned.

In measuring anode-flux voltage drops, a 0 - 1V shielded meter was employed in conjunction with two mild steel pointed probes. Two voltage drops were measured, one from the centre of the anode bus-bar to a point in the flux mid-way between the two central anodes on one side of the furnace, and the other from the anode bus-bar to the surface of one of the central anodes below the flux surface. The difference between the two values obtained corresponds to the voltage drop across the anode-flux interface from the anode surface to a point in the flux approximately 4in from the anode.

The first mentioned voltage drop was found to be 0.7 - 0.8V on a number of furnaces and was stable under normal operating conditions for the short period that measurements were made. The voltage drop from the anode bus-bar to the submerged anode surface was 0.45 - 0.5V, and represents a constant and permanent feature of cell design at present.

Thus, the interfacial voltage drop is of the order of 0.2 - 0.3V when the reduction furnace is operating normally. It is this component of the overall cell voltage that is capable of being lowered as a result of improving the physical and electrical contact between anode and electrolyte.

(b) Industrial Implementation

It has been mentioned in the introduction that the work described in this thesis has been undertaken partly as an applied study in the aluminium smelting process. With this aim in view, it is relevant to assess the results of the project in terms of their implementation in this process.

In probable order of practical importance, the following benefits have been sought:

1) A reduction in overall cell voltage.

2) A savings in power consumption per unit weight of metal produced.

3) A reduction in carbon usage per unit weight of metal produced.

4) A continuous means of adding raw materials to the reduction cell.

In terms of electrolyte requirements, the elimination of composition variables aids in achieving a constant cell voltage, with increased energy efficiency for the reduction process. A continuous system of raw materials addition is needed to maintain a constant electrolyte composition, and addition through the anode material is a practical means of achieving this end.

Equating carbon consumption to raw material needs determines the amount of a given additive which is required to keep a constant electrolyte composition, and thus the maximum permissable percentage of additive in an anode can be calculated. This procedure indicates that aluminium fluoride and cryolite, on the basis of a usage of 0.025 parts of each per unit weight of aluminium produced, can be added to carbon anode in amounts up to 5%. The figure for calcium fluoride is approximately 1%. It is not feasible to add all of the alumina requirements of the electrolyte as part of the anode, as the ratio of alumina consumption to carbon consumption approaches 4.0, and such an anode composition would prove unsuitable in practice. However, Watanabe

and Ōba (24) have shown that amounts of up to 50% alumina in carbon anodes have advantages in lowering the cell voltage and increasing the anode critical current density in laboratory cells.

Reduction in cell voltage can, on the basis of the foregoing work, be achieved with small amounts of anode additives, and the technological advantages of improved power and carbon consumption have been demonstrated.

The considered benefits and their means of implementation have been summarized (25) in a current Patent Application.

ACKNOWLEDGEMENTS

In conclusion, I wish to express my thanks to those who have shown readiness to assist in this project in a number of ways.

To Professor H. Bloom of the University of Tasmania, for his valuable supervision and guidance throughout the duration of the work, and the interest he has shown in the practical application of this project.

To the Management of Comalco Aluminium (Bell Bay) limited, for the provision of experimental facilities and permission to submit this thesis for higher degree purposes.

To Messrs. F.J. Strong and I.F. Bainbridge of Comalco, for their assistance in making it possible to undertake this work in the first instance, and for their helpful interest and encouragement throughout its various phases.

To Professor K. Grjotheim, of the Technical University of Norway, for valuable discussions and permission to reproduce the phase diagram of the $NaF-AlF_3$ system.

Finally, to my wife, who has painstakingly typed this report, and has patiently tolerated my moments of technological reflection when I have been unaware of her presence.

Osborne.

REFERENCES.

1. JANAF Thermochemical Tables, Dow Chemical Co., Midland, Michigan. 1964.

2. Wleugel, J., and Bockman, O., J. Electrochem. Soc., 101, 1456, (1954).

3. Welch, B.J. and Richards, N.E., "International Symposium on the Extractive Metallurgy of Aluminium", New York, 1962, Vol. 2, 15 - 29.

4. Welch, B.J., Proc. Aust. Min. & Metall., 1965, 1 - 19.

5. Thomstad, J. and Hove, E., Canadian Journal of Chemistry, July 1964, 42, (7), 1542 - 1550

6. Vajna, A., Meeting of the 3rd section of the Societe Francaise des Electriciens, 1950.

6a. Belyaev, A.I., Elektrolit alyuminievykh vann. Metallurgizdat, Moscow 1961.

6b. Matiasovsky, K., et al; Chem. zvesti, 17, (1963), 181.

7. Fedotieff, P.P., and Iljinske, W., Zeit. anorg. Chem., 80, (1913), 113.

8. Puschin, N., and Baskow, A., Zeit. anorg. Chem., 81, (1913), 347.

9. Lorentz, R., Jabs, A., and Eitel, W., Zeit. anorg. Chem. 83, (1913), 39.

10. Hardouin, M., Publ. sci. et tech. ministère air (France) Paris 1933, p. 34.

11. Grjotheim, K., Holm, J.L., Krohn, C., and Thornstad, J. "Selected topics in high temperature chemistry." pp. 151 - 178, (Oslo, 1966.)

12 Rollin, M., Meeting of the 3rd section of the Societe Française des Electriciens, 1950.

13. Førland, T., Storegroven, H., Urnes, S., Alluminio, 22, (1953), 631.

14. Treadwell, W.D., Schweiz. Arch. angew. Wiss. u. Tech., 6, (1940), 69.

15. Boner, J.E., Helv. Chim. Acta, 33, (1950), 1137.

16. Grünert, H., Z. Elektrochem., 48, (1942), 393

17. Bloom, H., Private Communication.

17a. Grjotheim, K., Holm, J.L., Krohn, C., and Matiasovsky, K. Svensk Kemisk Tidskrift, 78, 10, (1966), 547 - 567.

18. Zhemchuzhina, E.A., et al., Tsvetnaya metallurgiya, (3), 93 - 99 (1964), U.S.S.R.

19. Hollingshead, E.A. and Braunwarth, V.A., International Symposium on the Extractive Metallurgy of Aluminium, New York, 1962, Vol. 2, 31 - 50

20. Thonstad, J., J. Electrochem. Soc., 3(8), 1964, 959 - 965.

21. Henry, J.L., and Feinleib, M., "Physical Properties of Aluminium Reduction Cell Bath". K.A.C.C. Report No. CP56-4, May 23, 1956.

22. Welch, B.J. and Snow, R.J., Proc. Aust. Inst. Min. and Metall., March, 1967. 43 - 49

23. Evans, R.C., "An Introduction to Crystal Chemistry", 2nd edition.

24. Watanabe, N., and Ōba, N., paper presented at C.I.T.C.E. meeting, September 1966, Japan.

25. Bloom, H., and Osborne, J.A., Patent Application "Anodes for Electrolytic Production of Aluminium and Aluminium Alloys", May 23, 1966.

26. Handbook of Chemistry and Physics, Chemical Rubber Publishing Co., 43rd ed., 1961 - 1962.

27. Wranglen, G., Jernkont, Ann., 142, (1958), 10, 613 - 635.

APPENDIX "A": ANALYTICAL PROCEDURES.

The following details outline the analytical methods referred to throughout the text:

(a) Determination of Silicon in Fluorides.

0.4 g sample is fused with 1.0g borax to obtain a clear melt. The melt is extracted with nitric acid, 4ml ammonium molybdate added to the volume made to 50ml with deionized water. The determination is completed spectrophotometrically, and the silicomolybdate colour compared with calibration data after subtraction of the usual reagent blank.

(b) Determination of Iron in Cryolite and Calcium Fluoride

5g sample is digested with hydrochloric acid for 15 minutes and filtered. The filtrate, containing the iron, is reduced with stannous chloride and the determination is completed volumetrically using potassium dichromate solution and sodium diphenylamine sulphonate indicator. Pure iron is used as a standard.

(c) Determination of Iron in Aluminium Fluoride.

5g sample is fused with 30g potassium hydrogen sulphate, and the melt extracted in hot water. After acidification with hydrochloric acid, the determination is completed in the same manner as above.

(d) Aluminium in Aluminium Fluoride.

1g sample is fused with 5g potassium hydrogen sulphate and the melt extracted with hydrochloric acid. The resulting solution is made to 200ml with deionized water, and suitable aliquots withdrawn for the usual R_2O_3 precipitation and ignition. The aluminium content is then calculated from the gravimetric results.

(e) Aluminium in Cryolite.

A similar procedure to the above is used, except that the sample is fumed to dryness with sulphuric acid, and the residue then extracted with hydrochloric acid.

(f) Sodium in Cryolite.

From the same solution prepared for the determination of aluminium in cryolite, a suitable aliquot is withdrawn and evaporated to incipient dryness. The sodium content of the sample is then determined gravimetrically by treating the residue with a large excess of zinc uranyl acetate reagent and weighing the precipitate as sodium zinc uranyl acetate.

(g) Bath Ratio in Cryolite and Furnace Electrolyte.

The term "bath ratio" refers to the weight ratio of sodium fluoride to aluminium fluoride in the sample, and is an important operating variable in the control of industrial aluminium furnaces.

The analysis is performed by digesting 0.5g of

sample with 2% sodium hydroxide and adding a known volume of standard sodium fluoride solution. Part of this combines with the excess aluminium fluoride which is normally present in furnace electrolyte, and the cryolite so formed precipitates after acidification. The excess sodium fluoride is determined volumetrically with standard ferric chloride solution, using potassium thiocyanate as an indicator in an ether layer.

(h) Free Alumina in Cryolite and Furnace Electrolyte.

A 1g sample is boiled with 30% aluminium chloride solution to dissolve all fluoride materials. The undissolved alumina is retained on a small amount of paper pulp, and filtered off. The alumina is determined gravimetrically in the washed and ignited residue, after subtraction of a blank value.

(i) Calcium Fluoride in Furnace Electrolyte.

A 0.5g sample is fumed to dryness with sulphuric acid, and the residue digested in hydrochloric acid. After ammonia precipitation of group III metals, the filtered solution is made to a standard volume and the calcium fluoride determined flame photometrically.

(j) Calcium in Calcium Fluoride.

A 0.5g sample is fumed to dryness with sulphuric acid and group III metals removed from the hydrochloric acid solution of the residue by ammonia precipitation.

The filtrate is made to a standard volume, and the

calcium precipitated from an aliquot using ammonium oxalate. The washed calcium oxalate is dissolved in 10% sulphuric acid and titrated hot with potassium permanganate which has been standardized with solid sodium oxalate.

(k) Iron in Calcined Alumina.

A 2.5g sample is fused in a sodium carbonate-boric acid flux, and the chilled melt dissolved in deionized water. After reduction of the iron with hydroxylamine hydrochloride, the colour is developed with o-phenanthroline and its intensity read spectrophotometrically, deducting a reagent blank.

(l) Silicon in Calcined Alumina

A 2.5g sample is fused as above and similarly extracted in deionized water when cool. After pH adjustment, ammonium molybdate reagent is added, and the reduced silicomolybdate formed by reduction with stannous chloride. The intensity of the blue colour is read spectrophotometrically, deducting a reagent blank.

(m) Soda in Calcined Alumina.

A 0.5g sample is extracted with hydrochloric acid in a sealed tube at 200°C. The extract is made up to a standard volume, and the determination is completed flame photometrically.

(n) Specific Gravity of Anode Mixtures.

A sample of the anode material, either "green" or baked, is weighed in air, and then immersed in water overnight to expel air from the pores.

The sample is then removed from its container, surplus water dried off, and the sample weighed. A final weighing of this sample in water is performed, and from these three weighings the porosity, apparent specific gravity, and real specific gravity can be determined.

(o) Softening Point of Pitch Binder.

The cube-in-air method can be used for pitch materials with a softening point greater than about 80°C. A sample of pitch is melted to free it from air bubbles, and poured into warm moulds such that, after trimming, a ½in cube results, containing a small hole 1/16in diameter, and ¼in deep. This accepts the supporting wire which holds the sample in the air-bath of the apparatus. This air-bath is surrounded by a second vessel, and, after gas-heating from the base of the apparatus, the softening point is recorded as the temperature at which the sample falls from its supporting wire, as measured by a mercury-in-glass thermometer mounted adjacently. Duplicate samples are run concurrently.

(p) Resistivity of Anode Materials.

The sample to be tested is ground to -35 + 65 mesh Tyler and air-blown to remove finer material. Sufficient sample to form a cylinder 1in diameter and approximately 1in high is retained between circular electrical contacts in a ceramic tube. After compression of the sample to 150lb/sq.in, its resistance is measured using a bridge ohmmeter. Knowing the sample height from a dial gauge reading, the resistivity of the material can be calculated, allowing for a correction value due to the instrument.

APPENDIX "B": MISCELLANEOUS ANODE PROPERTIES.

Although power consumption and net carbon usage are significant factors in the economic production of aluminium, the suitability of the anode material in practice is influenced by a number of properties. Among those properties which may be readily studied in the laboratory and, in the present work, related to the nature and amount of additive in the anode are specific resistance, mechanical strength, specific gravity, and resistance to non-electrolytic oxidation.

To measure the effects of the various additives on the above properties, the following work was undertaken:

(a) Specific Resistance.

Standard procedure (p) in Appendix "A" was employed on a selection of anodes, so that the effects of the additives could be studied within their practical composition range in the sample. Using this method, the following results were obtained for plain and modified anode samples:-

Additive in unbaked anode	Ash content of sample under test	Specific Resistance (ohm - inches)
Nil	0.8%	0.0333
1.7% Al_2O_3	1.7%	0.0375
4.1% Al_2O_3	2.9%	0.0307
8.3% Al_2O_3	7.5%	0.0352
16.6% Al_2O_3	14.0%	0.0439
27.0% Al_2O_3	18.1%	0.0612
40.4% Al_2O_3	30.0%	0.1305
1.7% CaF_2	22.3%	0.0305
1.7% LiF	22.0%	0.0331
1.7% AlF_3	1.5%	0.0368
1.7% Na_3AlF_6	1.2%	0.0386
1.7% $CaCO_3$	2.8%	0.0350
1.7% Li_2CO_3	1.5%	0.0363
1.7% Na_2CO_3	2.4%	0.0338
Nil	1.6%	0.0354
1.7% Al_2O_3	2.4%	0.0382
4.1% Al_2O_3	3.1%	0.0401
8.3% Al_2O_3	4.1%	0.0416
16.6% Al_2O_3	9.3%	0.0461
40.4% Al_2O_3	30.1%	0.0978
1.7% AlF_3	1.7%	0.0393

The first group of results refers to anodes which were prepared for use in the laboratory reduction cell; the second group refers to samples prepared for compressibility tests, the residues being further pulverised for additional specific resistance measurements.

Measurements taken from plant records show that over one ten-month period the specific resistance of samples of large plant anodes, when measured by the same method, lay in the range 0.0308 - 0.0374 ohm - inches.

It may be concluded that only those samples containing relatively large amounts of additives are likely to be unsuitable as production anodes. (The specification limit for raw materials of this type is 0.045 ohm - inches.)

The explanation of rapid increase in specific resistance of the anode samples at levels of above about 15% of alumina has been previously discussed (this work, Part II Section (e)) in terms of the discontinuities in the carbon matrix brought about after void spaces have been filled by additives.

In the above table, partly reproduced in the graphs overleaf, the ash contents are in some cases lower than the amount of additive contained in the uncrushed sample. The cause of this is thought to lie in the crushing of the anodes, when some fine material is lost.

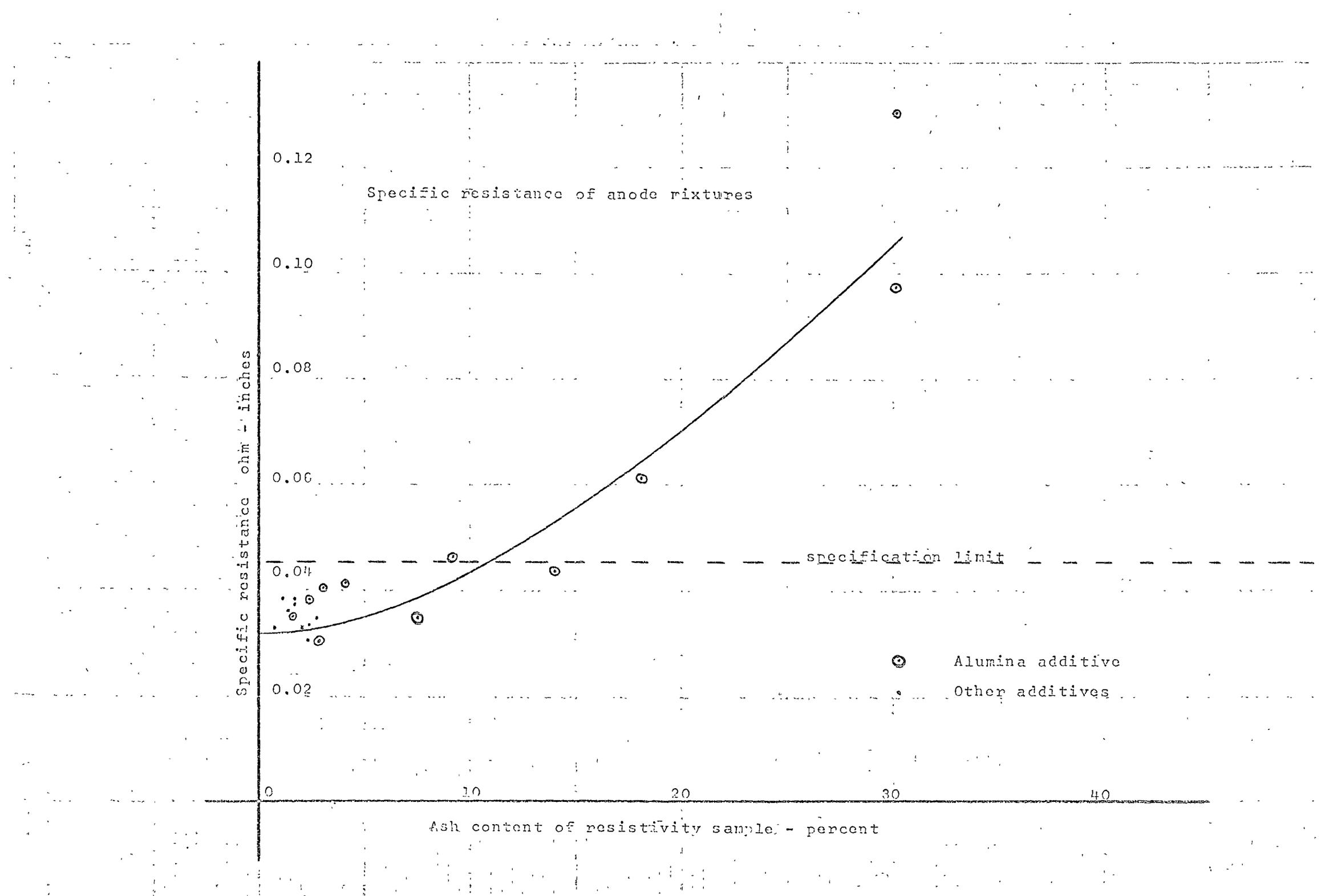
Specific resistance of anode mixtures
Specific resistance - ohm - inches
0.12
0.10
0.08
0.06
0.04
0.02
specification limit
Alumina additive
Other additives
0
10
20
30
40
Ash content of resistivity sample - percent

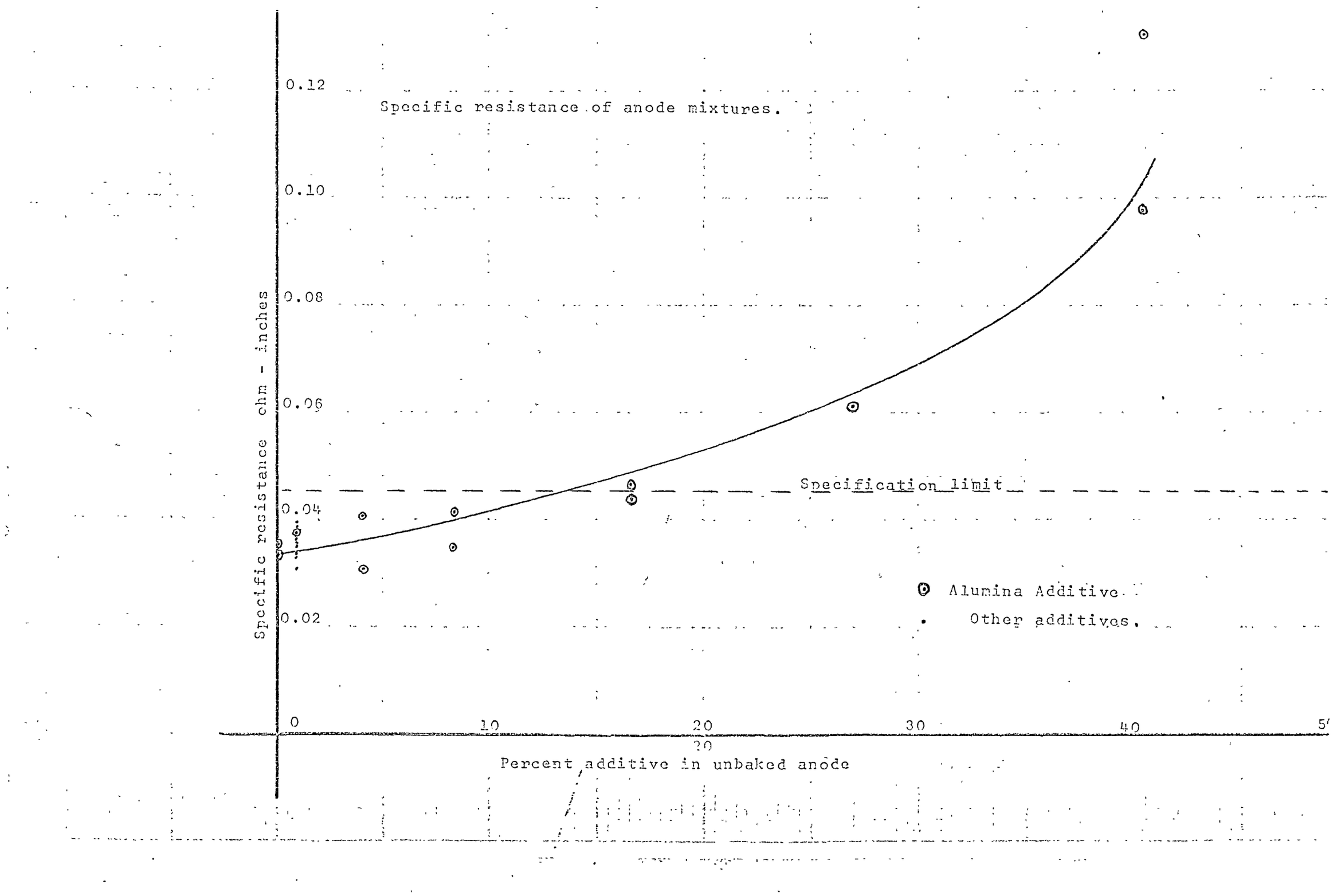
Specific resistance of anode mixtures.
Specific resistance ohm - inches
0.12
0.10
0.08
0.06
0.04
0.02
Specification limit
Alumina Additive
Other additives.
0
10
20
30
40
Percent additive in unbaked anode

This fraction would be expected to contain a proportionately larger amount of additive, considering that these additives have a finer overall particle size than the anode carbon.

Nevertheless it can be said that amounts of up to approx. 15% of the additives listed can be tolerated without large changes in the specific resistance of the block. In any event, the requirements of flux composition, when related to carbon consumed electrolytically, limit the amount of some additives, such as aluminium fluoride and cryolite, to five percent, with a much lower figure in the case of calcium fluoride.

(b) Mechanical Strength.

Measurements of compressive strength were made on cylindrical samples of baked anode material 1in in diameter and 2in long, using the Mohr and Federhaff equipment referred to previously. The sample was centrally located in an upright position on the lower plate of the apparatus, and the pressure increased at a constant rate until fracture occurred.

The results of these measurements are tabulated below:-

Sample No.	Additive in sample	Mean Compressive Strength (lb/in^2)
1	Nil	1862
2	2% Al_2O_3	1783
3	5% Al_2O_3	2249
4	10% Al_2O_3	2526
5	25% Al_2O_3	1598
6	50% Al_2O_3	2852
7	2% AlF_3	1808

The variations in the above table are considered to be caused mainly by differing amounts of pitch binder in the unbaked mixtures. In samples 1, 2, 3, and 7, approximately 14% of the total unbaked mixture consisted of pitch binder, samples 4 and 5 contained 16.8% of pitch, and sample 6 contained 21.9%. These variations in amount of pitch binder were based on previous experience in preparing high alumina blocks, and the compression tests show that it is possible to prepare a strong anode containing a high proportion of non-carbonaceous constituent. The lower compressive strength of sample 5 is considered to be due to insufficient binder for the amount of alumina additive in the mixture.

(c) Specific Gravity.

Samples of anode mixtures similar to those used in (b) above, were taken to measure the effect of large

amounts of additive on the specific gravity of the final baked cylinder. The method used is outlined in Appendix "A" (ń), and the results lay in the following ranges:-

Apparent S.G.	1.062 - 1.224
Real S.G.	1.430 - 1.775
Porosity	24.15% - 32.69%

Although the apparent specific gravity and porosity show variations as a result of minor changes in pressing conditions, there is a trend upwards in real specific gravity of the samples as the alumina content increases. This is as expected, as the specific gravity of calcined alumina is 3.95 - 4.0 (23) for the corundum form.

(d) Resistance to non-electrolytic oxidation.

During its lifetime in a reduction furnace, a pre-baked carbon anode is subjected to a degree of atmospheric oxidation unless precautions such as metal spraying or ceramic coating are taken.

The work of Wranglen (24) has shown that a number of inorganic compounds act as inhibitors to the atmospheric oxidation of carbon. Among the compounds which act in this manner are aluminium oxide and aluminium fluoride, while lithium and sodium carbonates, and cryolite, act as oxidation catalysts. The catalyst levels used in Wranglen's work were less than one per cent

in the carbon sample, whereas higher amounts of additives have been used in the present study.

To compare oxidation rates of plain and modified anodes, cylindrical samples 1in diameter and approximately 1½in long were prepared and weighed, a slice having been removed from each sample for ash determination. The samples were then placed upright in an electric muffle furnace for 1 hour at 800°C. At the end of the run, the samples were cooled and weighed, and the percentage of carbon which had been ashed away was calculated.

Percentage of Carbon airburnt at 800°C for one hour.

Additive in anode	% of Carbon oxidised.
Nil	29.0
2% LiF	26.5
2% Li_2CO_3	28.7
2% Na_2CO_3	28.3
2% CaF_2	26.6
1% CaF_2	27.8
2% $CaCO_3$	27.8
25% Lurgi dust	25.5
50% Lurgi dust	32.7
1% Al_2O_3	28.7
2% Al_2O_3	29.5

In the Lurgi dust samples, the use of higher than normal amounts of pitch binder prevented crumbling of the ashed sample, and the original shape of the cylinder was retained after ashing. In the case of the sample containing 50% of this material the higher percentage of carbon oxidized is thought to be due to a more porous sample in this case allowing more rapid oxidation of the carbon in the anode.

Apart from this single instance, the remaining figures for the amount of carbon oxidized are of the same order. It can be confidently predicted that atmospheric oxidation of anodes containing the amounts of additives mentioned above will not be more rapid than that of unmodified carbon.